EROSION ANALYSIS OF HYDRO TURBINE MATERIALS

A DISSERTATION

*Submitted in partial fulfillment of the
requirements for the award of the degree
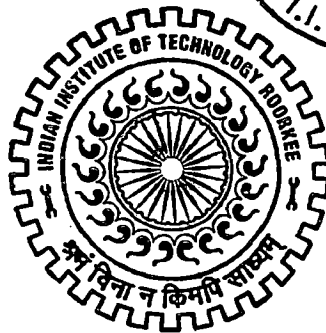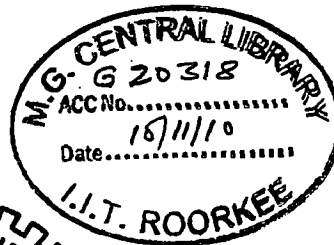of*

MASTER OF TECHNOLOGY

in

ALTERNATE HYDRO ENERGY SYSTEMS

By

KULDEEP SINGH SHEKHAWAT

ALTERNATE HYDRO ENERGY CENTRE
INDIAN INSTITUTE OF TECHNOLOGY ROORKEE
ROORKEE-247 667 (INDIA)
JUNE, 2010

CANDIDATE'S DECLARATION

I hereby certify that the work which is being presented in this dissertation, entitled, " **EROSION ANALYSIS OF HYDRO TURBINE MATERIALS**", in partial fulfillment of the requirement for the award of the degree of **Masters of Technology** in "**Alternate Hydro Energy Systems**", submitted in Alternate Hydro Energy Centre, Indian Institute of Technology, Roorkee is an authentic record of my own work carried out during the period from July 2009 to June 2010 under the supervision of **Dr. R.P.Saini**, Associate Professor, Alternate Hydro Energy Centre, and **Dr.Arun kumar** Head Alternate Hydro Energy Centre Indian Institute of Technology, Roorkee, India.
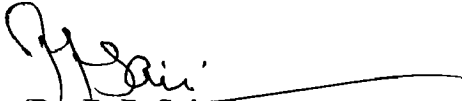
I have not submitted the matter embodied in this dissertation for award of any other degree.

Dated: June 28, 2010

Place: Roorkee

(KULDEEP SINGH SHEKHAWAT)

This is to certify that the above statement made by the candidate is correct to the best of my knowledge.

(Dr. R. P. Saini)	**(Dr.Arun kumar)**
Associate Professor	Head
Alternate Hydro Energy Centre,	Alternate Hydro Energy Centre,
Indian Institute of Technology,	Indian Institute of Technology,
Roorkee 247677	Roorkee 247677

i

ACKNOWLEDGEMENT

Dated : June/28/2010

(KULDEEP SINGH SHEKHAWAT)

ABSTRACT

In the Himalayan region main and suitable source of energy is hydro power potential of the resion . Many hydro plants have been in operation over last 50 years utilizing the hydro potential for electricity generation. Rain and snow fed rivers originating from Himalayas carries heavy amount of silt content almost 12000ppm which causes heavy erosion of turbine runner and other water part causing degradation of turbine efficiency over a period of time. Such erosive wear of hydro turbine runners is affected by silt size, hardness and concentration, velocity of flow in the turbine, angle of impact and base material properties. In the present study computational methodology has been used using commercial Finite Element Method (FEM) to calculate the erosive wear of different hydro turbines runner materials that may help to evaluate the performance of different materials for a particular type of silt contents. Different plots have been prepared showing erosion rate versus (velocity of water, angle of impact) that will help to choose the best turbine runner material according to site condition. High silt contents in river water has drastically reduced the power generating capacities of several power plants . The runner blade thickness can be reduced from 12-14 to 1-2 mm in a period of 6 months. The rebuilding of runners requires dismantling, transportation and recomissoing that required around 100 days of downtime for each generating unit . The loss of power generation capacity of up to 45% can be due to high silt wear of turbine runners. In silt water quartz content may be over 50%. Under the present Finite Element Method(FEM) approach has been considered. FEM tool is efficient and provides more relevant information about erosion.

In the present study

a) for analysis the erosion rate of turbine material 13Cr-4Ni ABAQUAS/EXPLICT software has been used.

b) An experimental study has been carried out for validation of the analyzed result on the slurry pot machine to perform the experiment the specimen of 13Cr-4Ni is taken.

c) By comprising the result of experimental study with FEM results it has been found that both result are comparable.

CONTENTS

CHAPTER 1   INTRODUCTION AND LITERATURE REVIEW

CHAPTER 2   SILT EROSION IN HYDRO TURBINE

CHAPTER-4 EXPERIMENTAL PROCEDURE AND TECHNIQUES

LIST OF TABLES

LIST OF FIGURES

NOMENCLATURE

SYMBOL	DEFINITION	UNITS
FEM	Finite Element Method	
W	Erosion rate	
A	Factor applied to plant capacity factor	-
B	Value of atmospheric pressure less water-vapor pressure at tailwater level (m of water head)	m
W	Erosion rate	
C_f	Plant capacity factor, equal to annual generation divided by (installed capacity x 8,760), expressed as a decimal, within a range of 0.1-1.0	-
C_g	Cavitation guarantee factor for a runner	-
D	Erosion constant	
E	Tail water elevation (above sea level)	m
g	acceleration due to gravity	9.81 m/s^2
h	Net head on turbine	m
k_1, k_2	Silt concentration fector	-
O	Turbine full-load output at rated net head	kW

C_1	Coefficient of silt concentration;	
C_2	Coefficient silt hardness;	
C_3	Coefficient of silt particle;	
C_4	Coefficient of silt particle shape;	
Mr	coefficient of wear resistance of base material	
R	Turbine runner factor	-
R_1	Revised turbine runner factor	-
T	Water temperature	^0C
V	Gross water velocity through throat of runner with no allowance for deduction of runner hub area	m/s
σ_p	Thoma coefficient	-
$NPSE$	net positive suction energy	Nm/Kg
E	specific energy	Nm/Kg
p_l	suction section pressure	Pa
ρ	density	Kg/m3

CHAPTER 1

INTRODUCTION AND LITERATURE REVIEW

1.1 INTRODUCTION

Energy is vital for sustaining on earth. Energy was, is and will remain the basic foundation, which determines the stability of economic development of any nation. It is needed to increase quality of life. Supply of energy for both biotic and a-biotic life support system is only possible by exploiting natural resources. The energy problem is, thus synonymous to ecological and economical problems. The gap between supply and demand of energy is continuously increasing despite of huge outlay for energy sector since independence. The total installed generating capacity of electricity in India 1, 59391.91 MW in May 2010 [33]. Among installed capacity, at present the largest share (>60%) was because of thermal electricity. Annual coal production was 240 million tons and crude oil production was approximately 32 million tons. Future energy demand in India is substantial as the 120% increase in annual oil production at 50 million tons, almost 250% increase in annual coal production at 600 million tones and doubling of natural gas production at 100 million cubic meters per day for the year 2012 [33]. This extraordinary growth in demand will place great stress on the financial, managerial and physical resources of the country, creating capital and energy shortages as well as environmental problems.

Since the post independence era the power sector in India has registered significant progress after the process of planned development of the economy began in 1950. Hydropower and coal based thermal power have been the main sources of generating electricity. Nuclear power development is at slower pace, which was introduced, in late sixties. The concept of operating power systems on a regional basis crossing the political boundaries of states was introduced in the early sixties. In spite of the overall development that has taken place, the power supply industry has been under constant pressure to bridge the gap between supply and demand. The demand for power in the country has been growing at the rate of 8% per year. The present installed capacity in the country is around 1, 59,391 MW as on May 2010 [33], 70% of which is supplied through fossil fuel (coal), about 25% through

hydro where as the nuclear power contributes a little less than 5% of the total power. The nuclear energy share in the world is 16%. The demand for electrical energy in India is rapidly increasing due to industrial and population growth,

The Indian power sector has made tremendous progress since independence in making power availability to widely distributed geographical boundaries of the country. However, due to various constrains, the demand always over stepped the power, resulting into power shortages in the past years. Hydro power is a renewable, economic and non-polluting source of energy. Hydro power stations have inherent ability of quick starting, stopping and load variations offering operational flexibility and help in improving reliability of power system. Hydro stations are best choice for meeting the peak demand. The generation cost is not only inflation free but reduces with time. Hydroelectric projects have long useful life extending over 50 years and help in conserving scarce fossil fuels. They also help in opening of avenues for development of remote and backward areas. Development of hydro power resources is important for energy security of the country.

For a fast developing country like India, the Govt. of India has planned to provide "power for all by 2012". As per the programmed approved by the planning commission, during the 11th plan period a capacity addition of 78,700 MW comprising 59,693 MW Thermal, 15,627 MW Hydro and 3,380 MW Nuclear and 14,000 MW Renewable and the addition of 90,000 MW during 12th Plan (2012-2017) constitutes 40,000 MW (Thermal), 30,000 MW (Hydro), and 12,200 MW (Nuclear) [33].

1.2 SMALL HYDRO POWER

Small hydro represents the 'highest density' resource and stands in the first place in generation of electricity from such sources throughout the world. Emanating from the environmental and depleting conventional sources consciousness, there is an increased thrust on small hydro development in India. Government of India has stimulated considerable enthusiasm in providing speedy development of small hydro. SHP acts as the small centers for power generation even in the remote areas where the basic needs of discharge and head are fulfilled thus emerging as an answer to the search for alternative energy source. India has a history of 100 years of Small Hydro since its first installation of 130 kW at Darjeeling in

the year 1897. India has one of the world's largest Irrigation Canal networks with thousands of Dams and Barrages. It has monsoon fed, double monsoon fed as well as snow fed rivers and streams with perennial flows. An estimated potential of about more 15,000 MW [1] of small hydro power projects exists in India. World installed capacity of small hydro today is around 50,000 MW against an estimated Potential of 180,000 MW. In India, out of 150,000 MW hydropower potential, 15,000 MW potential is estimated as small hydro, of which about 12% has been tapped so far. The present status of SHP in India is given in Table 1.1

Table 1.1 SHP status in India [33]

Overall potential	15,000 MW
Identified potential	10,477 MW (4,404 sites)
Installed capacity	1937 MW (581 projects)
Under construction	561 MW (207 projects)
Capacity addition during 2002-2007	Over 500 MW
Target capacity addition – 11th Plan (2007-2012)	1400 MW

In India, SHP schemes are classified by the Central Electricity Authority (CEA) as given in the Table 1.2

Table 1.2 Classification of hydro schemes in India [33]

Type	Station Capacity	Unit rating
Micro	Up to 100 kW	Up to 100 kW
Mini	101 to 2000 kW	101 to 1000 kW
Small	2001 to 25000 kW	1001 to 5000 kW

Power stations are also classified based on the head available and is given in Table 1.3

Table 1.3 Classification based on head [3]

Type	Range of Head
Ultra Low Head	Below 3 m
Low Head	3 to 40 m
Medium/ High Head	Above 40 m

1.3 TYPES OF SHP SCHEMES

Small Hydropower can also be broadly categorized in three types as follows:

1.3.1 Run-Off River Scheme

Run-of-River hydroelectric schemes are those, in which water is diverted towards power house, as it comes in the stream. Practically, water is not stored during flood periods as well as during low electricity demand periods, hence water is wasted. Seasonal changes in river flow and weather conditions affect the plant's output. After power generation water is again discharged back to the stream. Generally, these are high head and low discharge schemes.

1.3.2 Canal Based Scheme

Canal based small hydropower scheme is planned to generate power by utilizing the fall in the canal. These schemes may be planned in the canal itself or in the bye pass channel. These are low head and high discharge schemes. These schemes are associated with advantages such as low gestation period, simple layout, no submergence and rehabilitation problems and practically no environmental problems.

1.3.3 Dam Toe Based Scheme

In this case, head is created by raising the water level behind the dam by storing natural flow and the power house is placed at the toe of the dam or along the axis of the dam on either sides. The water is carried to the powerhouse through penstock. Such scheme utilizes the head created by the dam and the natural drop in the valley.

1.4 FORMULATION OF HYDRO POWER POTENTIAL

Hydro power is obtained from the potential and kinetic energy of water flowing from a height. The energy contained in the water is converted into electricity by using a turbine coupled to a generator. The hydro power potential of a site is dependent on the discharge and head available at the site. The Power is estimated by the following equation: [5]

$$\text{Power (P)} = \rho \times g \times Q \times H \times \eta_0 \qquad \text{Watts} \qquad (1.1)$$

where, ρ is density of water, g is acceleration due to gravity, Q is discharge in m^3/s, H is head in m and η_0 is overall efficiency of the turbine, generator and gear-box.

The head is relatively constant in run-of-river schemes except for variation in friction losses, with the varying discharge. Whereas, in canal based and dam toe based schemes head also varies depending on water releases and season of release. The design head is so selected that turbine is operated to the maximum time giving optimum energy generation. Energy generation per year is given as:

$$\text{Energy Generation per Year} = \text{Power (kW)} \times \text{Time in hours per year} \qquad (1.2)$$

1.5 DIFFERENT COMPONENTS OF SHP

The schematic diagram of Run-off River (ROR) hydropower plant and also the arrangement of different components of SHP are shown in Fig. 1.7.

i. Civil works components

ii. Electro- mechanical equipments

1.5.1 Civil Works Components

The purpose of civil work components is to divert the water from stream and convey towards the power house. In selecting the layout and types of civil components, due consideration should be given to the requirement for reliability.

5
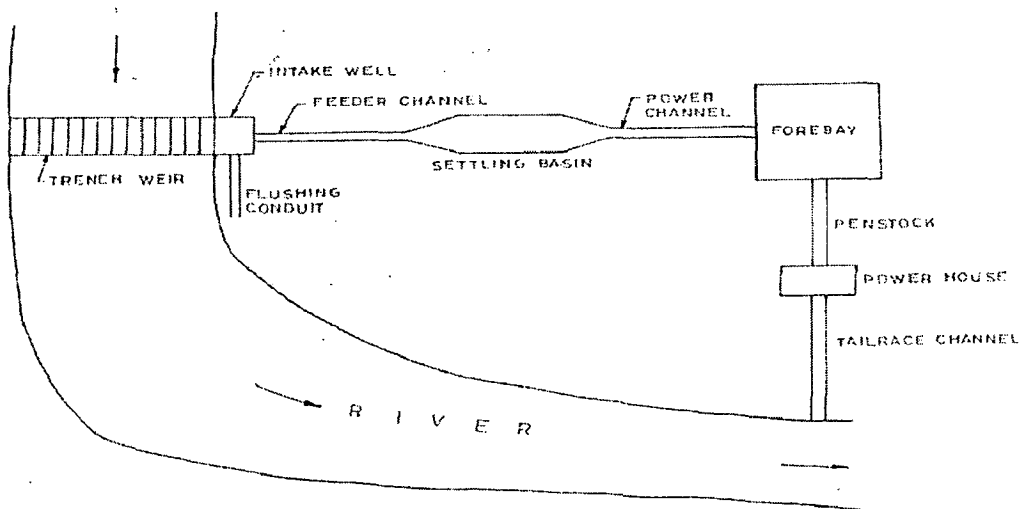
Fig. 1.1 Schematic diagram of run-off river plant [6]

1.5.2 Electro Mechanical Equipments

Electro-Mechanical equipments mainly include hydro turbine, generator, speed increaser, governor, gates and valves and other auxiliaries.

1.6 LITERATURE REVIEW

Asthana [1] proposed that The turbine abrasion was expressed as

$$TA = f(PE\, v^z) \tag{1.3}$$

Where PE is modified suspended sediment content, v is relative velocity between flowingwater and turbine parts where abrasion is severe, and z is exponent for relative velocity.The modified sediment content (PE) is expressed by the following equation:

$$PE = P^\alpha a^\beta k_1\, k_2\, k_3 \tag{1.4}$$

Where P is the average annual suspended sediment content in gm/l. It is based on the longterm measurements in the river; α is exponent of 'P' representing correction factor for suspended sediment concentration. It is taken as 1 for concentration up to 5 g/l; a is average grain size coefficient of suspended sediment with a base of 0.05mm; β is exponent of 'a' representing correction factor for average particle size, which was taken as 1 for particle up to 0.6mm and curved flow; k1, k2, k3, represent the coefficient to account for shape,

6

hardness and abrasion resistance of base metal, respectively. k1 is taken as 0.75, 1.0 and 1.25 depending on irregularities ranging from few to severe, k2 was taken as 1 for hardness greater than 3 (on Moh's scale) and 0.5 for less than 3, k3 was taken as 1 for 13Cr4Ni steel.

Schneider et al.[2] proposed that wear rate, W was a function of a multitude of parameters as shown in the following algebraic relation:

$$W = c\, q\, f\, d_{50}\, v_f^n \tag{1.5}$$

Where c (kg/m3) is sand concentration, q (kg/kg) is hard particle contents, d_{50} (m) is median particle size, and v_f (m/s) is flow velocity. The authors suggested that the value of n varied considerably from about 2.1 to more than 3. This range of values was reported to reflect the limitations of the algebraic relation, which considered neither the material parameters of the eroded body nor the flow parameters or the various material parameters of the silt particles.

Mack et al. [3] suggested a numerical model to predict the erosion on guide vanes andon labyrinth seals in hydraulic turbines. The prediction of erosion, based on the Lagrangian calculation of particle paths in a viscous flow, was described for two components of a Francis turbine, for which results of field tests were available. It was shown that the erosion level was strongly dependent on the particle size. A fully 3D flow and erosion calculation around the guide vanes of the same Francis turbine was presented. It was shown that the geometry of the guide vane including tip clearance, support and fillets lead to a complex flow field, which, as a consequence, resulted in a complicated fluid–particle interaction strongly affecting the erosion pattern. There was a good agreement between the numerically obtained erosion pattern and the field test measurements.

Keck et al. [4] presented a study on the utilization of CFD method to predict the erosion pattern in a hydraulic turbine and compared it with field measurements of the erosion. Sand erosion was modeled by applying the Lagrange method i.e. tracking a large number of individual particles in the flow field. The motion of the particles was described by the Basset–Boussinesq–Oseen equation whereby experimentally based correlations were used for the drag and the influence of turbulent motion. During the Lagrangian tracking, the number of particles impinging on a surface was recorded. Out of these data the removal of the wall was calculated. Calculations were performed for different particle sizes. The result showed a

7

good correlation for the erosion pattern with the field observation. However, the authors concluded that CFD simulation did not provide accurate absolute erosion, although it could be used to obtain relative erosion intensities and to evaluate different designs relative to each other.

R. Chattopadhyay [5] found extremely high wear of cast CABNM hydro turbine runners due to high silt contents in river water has drastically reduced the power-generating capacities of several power plants . The runner blade thickness can become reduced from 12-14 to 1-2 mm in a period of 6 months. The rebuilding of runners requires around 100 days of downtime for each generating unit every year. The loss of power generation capacity of up to 45% can result from the high silt wear of turbine runners. The silt content can be as high as 5000 ppm. The quartz content of silt is around 50%. The objective of this study is to identify suitable alloys which when used as weld overlays should minimize high silt wear. The alloys selected are stellite 6 type, 316L stainless steel and 15wt.% Cr-1Swt.% Mn steel. Stellite 6 and 15wt.% Cr-1Swt.% Mn stainless steel are known for their excellent wear resistant properties in an erosion-cavitation type of situation. Type 316L stainless steel has been selected for its purely austenitic structure, good weldability with a CA6NM-type base and superior pitting resistance. The results of slurry erosion tests are A. The wear rate of Stellite 6 is the least followed by 15wt.% Cr-1Swt.% Mn stainless steel. The wear rate of type 316L is higher than that of CABNM. The results are obtained from three types of experiment, namely, liquid impact erosion, cavitation and field tests.

Chauhan et al. [6] the martensitic stainless steel (termed as 13/4) is currently being used for fabrication of underwater parts in hydroelectric projects. There are, however, several maintenance problems associated with the use of this steel. A nitronic steel (termed as 21–4–N) has been developed as an alternative with the specific aim of overcoming these problems. A comparative study has been made on the erosion behaviour of 13/4 and 21–4–N steels by means of solid particle impingement using gas jet. The eroded surfaces after erosion tests were analysed by scanning electron microscopy. It is observed that the 21–4–N nitronic steel possesses better resistance to erosion in comparison to 13/4 martensitic stainless steel. The

austenitic matrix of the nitronic steel possesses high hardness, high tensile toughness and work hardening ability, which results in higher erosion resistance.
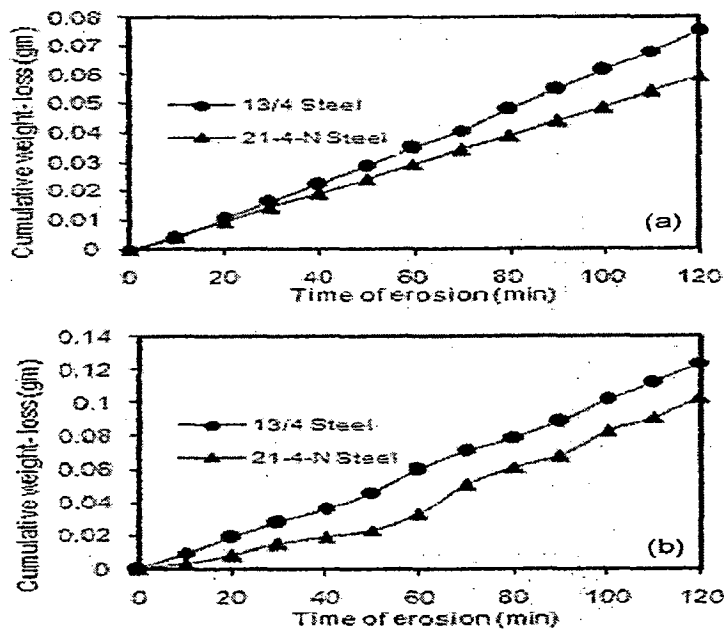
Figure 1.2 Cumulative weight loss as a function of erosion time at impingement angles of (a) 30° and (b) 90°.

i.   The erosion resistance of 21–4–N nitronic steel investigated by means of solid particle impingement is higher than that of 13/4 martensitic stainless steel.

ii. High erosion resistance of 21–4–N steel is due to the distribution of hard carbides in the matrix of stabilized austenite.

iii. Mechanical properties significantly affect the erosion resistance of target material. In 21–4–N nitronic steel, high resistance to erosion is due to high hardness

H.P. Neopane et al.[7] proposed an alternative design of a Francis turbine for minimizing the sand erosion effect in sand laden river. To achieve this objective, one erosion model for hydraulic machinery has been selected and all technical and managerial aspects suppose to be considered in this study. Hydraulic turbine components operating in sand-laden water subject to erosive wear. Erosion reduces efficiency and life of turbine. It also causes problem in

9

operation & maintenance. Himalayan rivers carry large amount of hard abrasive particles. Withdrawal of the clean water from the river for power production is expensive due to design, construction and operation of sediment settling basins. Even with the settling basins, 100% removal of fine sediments is impossible and uneconomical.

V.K. Pande [8] In India, 80% of available Hydro resources are from Himalayan region. Silt erosion of Hydro turbines is a widely acknowledged problem. Problem is severe in the Himalayan region because the mountains are young and relatively fragile. Silt and damage depend on nature of silt, quartz rich with quartz content generally 65%-95%, PPM content high: 5000 to 20000 in monsoon, freshly broken fine conical particles. Due to silt damaged areas guide vane and Cheek plate, runner inlet at blade skirt and crown, runner outlet on pressure side, pelton nozzle & Spear, pelto runner bucket.

B.S. Mann [9] discussed problem of erosion due to silt in a number of Indian hydro power stations is found to be quite serious, especially in those located in the Himalayan region. Erosion is a function of different parameters such as silt size, hardness, concentration, quantity, shape, velocity and base material properties. In most cases, this can be minimized by controlling the above-mentioned parameters. During monsoon season, it becomes impossible to control these parameters which cause erosion. So, it is essential to know their effects. Wear, which occurs due to low and high-energy particle impact, can be controlled by velocity or by controlling silt size, shape and concentration. The low energy impact wear can also be controlled by providing suitable hard coatings. However, this becomes critical for high particle impact wear. An experimental study was undertaken for understanding its nature. In this study, hard coatings such as hard chrome plating, plasma nitriding, D-gun spraying and boronising were studied for high-energy impact wear resistance. Boronising appears to be excellent for this, followed by D gun sprayed WCq12Co coating. Based on this experimental study, boronising is being field-tried on a component which is prone to erosion due to high-energy particle impacts. Under identical test conditions at high particle impact energy, the borided T410 steel performed much better than D-gun sprayed tungsten carbide as well chromium carbide, hard chrome, plasma nitriding and boronised 13Cr–4Ni steel. The borided T410 steel is free from cracks and voids. The microstructures of D-gun sprayed tungsten carbide and chromium carbide show a few voids and oxides as defects. At high

particle impact energy, thes defects could cause deterioration of the coating. The microstructure of borided 13Cr–4Ni steel also has defects such as cracks and these extend deep inside the coating up to the base and are responsible for unsatisfactory performance. The microstructures of hard chrome and plasma nitrided samples are free from all these defects. However, they lack the resistance to abrasive wear as their microhardness values are below the threshold values of the microhardness values of the erodent 1100 Borided T410 steel appears to be an excellent erosion resistance shield to combat highenergy particle impact wear. It can provide an appropriate solution to the hydropower stations severely affected due to silt and coming under categories A and B. Other coatings such as D-gun based, hard chrome and plasma nitriding may not provide an appropriate solution. This is because of their unsatisfactory performance in the laboratory.

Padhy and Saini [10] investigated the erosion damage is considered as the gradual removal of material caused by repeated deformation and cutting actions. Sand erosion is designated as abrasive wear. This type of wear will break down the oxide layer on the flow guiding surfaces and partly make the surfaces uneven which may also be the origin for cavitation erosion. Sand erosion therefore may be both a releasing and contributing cause for damages that are observed in power plants with a large transport of wearing contaminants in the water flow. The actual mechanism of erosive wear was not fully understood. Therefore, a simple, reliable and generalized quantitative model for erosion could not be developed. Most common expression for the erosive wear was based on experimental experiences. The hydro-abrasive wear was commonly quantified by means of wear rate W, defined by loss of mass per unit time. Silt erosion in hydro turbines cannot be avoided completely, but can be reduced to an economically acceptable level.

Kjolle [11] studied the causes of damages in hydro turbines and found that the main causes of damage of water turbines were due to cavitation problems, sand erosion, material defects and fatigue. The turbine parts exposed to cavitation are the runners and draft tube cones for the Francis, Kaplan and the needles, nozzles and the runner buckets of the Pelton turbines. The effect of cavitation erosion was found to be reduced by improving the hydraulic design and production of components, adopting erosion resistant materials and arrangement of the turbines for operations within the good range of acceptable cavitation conditions.

Neilson and Gilchrist [12] They Studied the total wear at normal impact angle assuming the total wear to be contributed by only deformation wear, which gives a deformation factor (€) as below:

$$\text{€}=Wd\ /1/2M(V\sin\theta-k)^2 \qquad (1.6)$$

Where Wd is deformation wear at normal impact condition, 'M' is the total mass of impacting particles, 'V' is velocity of particle, θ is impact angle and k is the normal component of particle impact velocity needed to initiate the erosion which is generally neglected, considering very small compared to the impact velocity.

Bain et al. [13] attempted to develop a correlation for the estimation of erosion rate based on extensive data collected in a bench scale test rig. The general form of the correlation can be represented as,

$$W=K\ V^\beta\ d^\psi\ C^\varphi \qquad (1.7)$$

Where W is erosion rate, V is velocity of particle, d is particle size, C is solid concentration, and K, β, φ and ψ are constants whose values depend on the properties of the erodent as well as the target material. For different erodents, the effect of particle size has been normally considered as a parameter affecting the wear and the exponent value was ψ found to lie between 0.3 and 1.6 .

Krause and Grein [14] reported that the abrasion rate on conventional steel Pelton runner made of X5CrNi 13/4 was as given below,

$$\delta=pqcv^{3.4}f(d_{p50}), \qquad (1.8)$$

Where δ is abrasion rate (mm/h), p is a constant, q is quartz content, c is mean sand concentration, and v is relative jet velocity; f(dp50) is function defining particle size. Since the above equation had been proposed for X5 CrNi 13/4, it is applicable to turbine components made of this material only. They carried model tests with varying parameters with the X5 CrNi13/4 steel, normally used in hydro plants. The test rig was designed to simulate the flow conditions in a turbine. A natural sand/water mixture taken from a power plant reservoir and sand containing 99% quartz in various grain sizes were used for the tests.

They have concluded that the abrasion rate is a function of velocity, sand content and proportion of hard components and size of the sand particles. The maximum abrasion occurred within an approximate particle size range of 40-70 mm.

Naidu [15] suggested the following expression for predicting the silt erosion rate:

$$W = S1 \, S2 \, S3 \, S4 \, M_r \, v^x \tag{1.9}$$

Where S1 is coefficient of silt concentration, S2 is coefficient of silt hardness, S3 is coefficient of silt particle size, S4 is coefficient of silt particle shape, Mr is coefficient of wear resistance of base material, and v is relative velocity of water.

Using erosive wear concept, detailed two-dimensional boundary layer profiles of simple circular objects and aerofoils at different Reynolds numbers under rotation have been obtained. The boundary layer profile of an aerofoil whose flight data using pitot static tube was available, was also compared. The boundary layer growth under rotation especially on pressure side of this aerofoil is substantially lower than actually obtained during flight. The observed region of separated zones and wake behind round objects and aerofoils are in good agreement with the data made available elsewhere. Under rotation the boundary layer thickness especially on pressure side is appreciable less because the favorable pressure gradient arises due to centrifugal forces acting on the fluid. These were practically observed on aerofoils and as well as on round objects. The boundary layer profiles of hydro, steam, and gas turbine blades, under simulated operating conditions, were taken. The boundary layer profile using viscous calculations for the objects under rotation can be compared. Generally, these calculations lack sufficiently detailed and precise data. Once the above data is available, the calculation scheme can be compared and this practical data will be of immense use for overall boundary layer characteristics for hydro, steam and gas turbines blades. This new concept can also be used for predicting erosion damages in hydro, steam and gas turbine blading. The experimental and theoretical erosion damages are in good agreement.

Padhy and Saini [16] found that the erosive wear rate increases with an increase in the silt concentration irrespective of the silt size. However, for a given value of silt concentration, the erosion rate has been found to be higher for larger size particles as larger particles have higher impact energy. Using experimental data a correlation for erosive wear rate was

developed as a function of particle size, silt concentration, jet velocity and the time of operation which has been found to have a good agreement with experimental data. The developed correlation may be useful for turbine manufacturing industry in order to predict the quantum of erosion in Pelton turbine bucket at manufacturing stage

Okamura and Sato [17] perform The hydraulic performance tests on a Francis turbine model with sediment laden flow, conducted in Japan and reported by Okamura and Sato , showed that the turbine's best efficiency decreased in direct proportion to the increase in solids concentration. The efficiency was correlated by the following expression:

$$\eta_m = (1 - .085 C_w)\eta_w \tag{1.10}$$

where is η_m turbine peak efficiency with sediment-laden flow, η_w is turbine peak efficiency with clean water, and C_w is fraction of solid by weight.

Sundararajan [18] presented a comprehensive theoretical model for erosion, valid for all impact angles combining the concept of localization of plastic deformation leading to lip formation and the generalized energy absorption relations valid for all impact angles and all shapes of eroding particles.

Roman et al. [19] reported the development of a new erosion resistant coating NEYRCO a composite coating with ceramic and organic matter base, designed to combine hardness and ductility. They carried out a series of model tests in a specially designed test rig to find the effectiveness of the coating against erosion. Four water velocities were used: 20, 25, 36, and 48m/s. The water flow rate was 2.5 l/s. The abrasive material was high silica content with the following chemical composition:

TABLE:1.4 Abrasive material composition taken by roman for his study[19]

SiO_2	>99.5%
$Al_{12}O$	>0.2%
Fe_2O_3	>0.2%
$CaCO_3$	>0.04%

Size	200–400 μm
Concentration	20 g/l

Surface examinations of the samples subjected to same erosive condition showed that the coated samples gave better performance as compared with the uncoated samples

Mann and Arya [20] studied the silt erosion characteristics of plasma nitriding and HVOF coatings along with commonly used steel in hydro turbines. The characterization of abrasive wear was carried out as per ASTM G-65. Angle of incidence, velocity and Reynolds numbers were maintained similar to those that commonly occur in hydro turbines, simulating low as well as high-energy impingement wear. The test parameters adopted are given below in table:

TABLE: 1.5 The test parameters adopted by Mann and Arya are [19]

1 kg mineral sand of hardness	1100HV
Size of erodent	180–250 μm
Erodent flow rate	5.5 g/s
Sample size	75mm x25mm x6mm

HVOF coating showed superior performance than plasma nitrided steel, but the demerits of HVOF coating was that it showed micro cracking, debonding and digging out of WC particles. For plasma nitrided steels there was ductile mode of erosion.

Engelhardt and Oechsle [21] examined different materials and coatings to evaluate their resistance to the hydraulic turbine surface. A hard, HVOF-applied TC/CoCr coating, named Diaturb 532 and a soft PU-based coating called Softurb 80 were chosen for testing. The samples were tested in a test rig. Later, the San Men Xia hydro power plant in China's Henan province was chosen for full scale testing of the improvements found during the laboratory research programme. The project included a monitoring phase of 2 years, during which the

turbine parts were inspected several times. Except for some mechanical damage to the protection systems, wear rates on the HVOF-coated runner blades were determined to be within the accuracy of the thickness measurement gauge (<40 mm). The wear rate on the PU-coated surface of the runner blades and the guide vanes was determined to be around 0.15mm per year. The unit was in operation during the 2-year monitoring phase and also during the flooding season with an average sand concentration of 20–30 kg/m3

Thapa and Brekke [22] carried out laboratory erosion experiments on curved specimens by particles of different size to simulate the flow in Pelton bucket in a high-velocity test rig. Aluminum specimens with different curvature were used for the testing. Baskarp-15 foundry sand with 66% free quartz (fine sand) of size 174 mm and artificial silica sand (coarse sand) of size 256 mm were used as the erosive particles. The results were presented in the form of erosion rate for different profiles and surface roughness at different locations of curved specimens. By visual observation of eroded particles the authors concluded that most of the coarse grains strike close to the splitter, whereas the fine grains were observed far away from the splitter. The erosion rate in terms of weight loss per unit striking particle found smaller with fine particles. This was due to low particle impact energy of smaller particles and might be because some of the fine particles escaped gliding without striking the surface. Another observation they made was erosion rate in mg/kg increased with the increase in curve radius.

Ahluwalia et al. [23] They suggested a number of measures such as providing adequate desilting arrangements, facilities for quick segregation and easy access to vulnerable parts, judicious choice of the type of turbine as well as operating speeds, use of stainless steel materials and availability of skilled maintenance staff to evaluate techno-economic considerations for hydropower stations in India. They also emphasized that the above recommendation can only reduce the erosion problem by extending the period between the shot downs but cannot eliminate the same in the underwater turbine parts totally.

Singh SC [24] reported the case study of the Tiloth hydropower station (3x30 MW) on river Bhagirathi. The three units were commissioned in 1984. The turbines were found to be seriously damaged after about 2600 h of operation. They were repaired, but extensive damage was observed again within 3000–5000 h of operation. The sedimentation chamber had been designed to arrest silt particles larger than 0.3mm. Petrographic studies carried out

revealed the presence of highly abrasive quartz, having hardness of 7 on Moh's scale. The concentration of the silt particles during the rainy season was maximum and reached up to 4000 ppm. Initially, there was a proposal to provide another sedimentation chamber to arrest particles up to 0.15mm. But due to very high cost and as the settling chambers could not completely remove the silt particles, the proposal was not implemented. The investigators, rather, suggested improving the metallurgy of the turbine blades. The new runner was manufactured with stainless steel (13 Cr 4 Ni), which was supposed to give a better performance regarding erosion. However, it was observed that there was no appreciable reduction in the erosion compared with the older runners.

Yan [25] studied the effect of silt abrasion in different hydropower plants of China and had drawn the following conclusions:

a) The abrasion remained moderate for all particles smaller than 0.05mm and rises sharply for larger sizes.

b) The product of operating head H and content of harmful sediment Sd (d40.05mm) must be less than 7, so that the abrasive erosion in the turbine would be minimum.

Kumar et al.[26] reported the case study of Tiloth Power station under Maneri Bhali Stage-I Project, which is basically a run-of-river scheme, at river Bhagirathi between Maneri and Uttarkashi (India). Detailed examination of runner blades of Unit-I revealed that there was thinning at outlet edges due to heavy erosion along with pitting marks before 1 year of commissioning. The analysis indicated that thinning of blade was caused by silt erosion. There was also heavy leakage of water from the guide vane bush housings. Subsequent inspection of under water parts revealed that the runner blades have been extensively damaged and big pieces of 300mm x350mm size has just sheared off. Further, visual examination revealed that there were more cracks near the skirt of the runner blades. In Unit-II and Unit-III, the extend of damage to the runner blades was similar to the damage noticed in Unit-I. Such an extensive damage is expected to be caused due to excessive silt, designed/operating condition, metallurgy of blades and inadequate design of runner profile.

Mathur et al.[27] reported the case study of Salal (6x115MW) hydropower station on river Chenab and Baira Siul (3x60MW) hydropower station on river Baira and Siul. The silt contents of the water of above rivers indicated the presence of 75–98% quartz bearing hardness 7–8 on Moh's scale and about 98% silt particles are of size 0.25mm and less. After 4000 h of operation at Baira Siul guide vanes made of 13Cr4Ni stainless steel, the loss was about 10–15% whereas at Salal this loss was approximately 10–12% of design weight. Stay vanes made of carbon steel get eroded. Pressure side of runner blades, crown and skirt get eroded very fast. In 2 years of operation runner profile gets altered. Labyrinth gap in Baira Siul increased from the design value of 0.8–1.2 to 3–4mm in only 1 year of operation. At Salal, lower labyrinth ring and sometimes portions of lower ring skirt get washed away in 8–10 thousand hours of operation of machines. Such type of erosion caused increase in the vibration level of machines at both power stations.

Wood et al. [28] reported a field study carried out by China North West Electric Power by mounting coated specimens in different places in Kaplan and Francis turbines and left during the flood season. Coated region had reduced the worn out thickness between 5 and 43 mm, whereas the surrounding uncoated metal had been worn down by between 1 and 10mm. The research programme concluded that minimum loss of efficiency can only be reached by a combination of design optimization, based on erosion prediction and protection of surfaces with wears reducing coatings.

Pradhan [29] observed during his studies that in run-of-river power plants in steep sediment loaded rivers the conventional design criteria to trap 0.2mm size sediment particles did not seem to function satisfactorily. In general, projects were having damages to runners due to severe erosion caused by silt. In case of Jhimruk Project, the wear on runner was so high that it required repair after every monsoon. A case study was carried out for JHP, a 12-MW run-of-river type project built and commissioned in 1994. The settling basins had been designed to trap 90%of 0.2mm size particles. During the sediment monitoring programme, the investigators observed that average values for suspended sediment concentration in Jhimruk river during the peak monsoon ranges from about 2000 to 6000 ppm with upper values ranging from about 20,000 to as high as 60,000 ppm, which indicated that the sediment transport in Jhimruk River during the monsoon was quite significant. The runners were

significantly worn out after every monsoon. From the damages observed in the runners it was revealed that the runners in the power plant were exposed to too much higher sediment load than expected during the planning and design stage. The author developed a correlation between sediment load to which the turbine was exposed to and corresponding decrease in efficiency of the turbine over a time period and concluded that the efficiency loss was 4% at best efficiency point and 8% at 25% load. The results from the thermodynamic efficiency measurements obtained during his studies

Thapa et al.[30] investigated the effect of suspended sediments in hydropower projects based on a case study of 60MW Khimti hydropower plant. Due to the presence of high amounts of sediments, the hydropower plant was designed with settling basins to screen 85% of all particles with a fall diameter of 0.13mm and 95% of all particles with a fall diameter of 0.20mm. The plant was commissioned in July 2000 and the damage to the turbine components was investigated in July 2003. The investigators had observed that a significant amount of erosion had appeared in the turbine bucket and needles. Even though the settling basins were performing satisfactorily, particles smaller than the design size passed through the turbines and caused the damage. The bucket thickness was reduced by about 1mm towards the root of the bucket, which is critical from the point of view of strength and hence the reliability of the component. Similarly, the splitter of the bucket was eroded to saw tooth form from the original straight edge. The sharp edge of the splitter had blunted and the width became approximately 4mm due to which the efficiency of the turbine had decreased. To minimize the effect of erosion hard ceramic coatings were applied on the bucket and needle surface at the cost of around US$ 25,000 per runner, but performances were not promising.

J.G.A. Bitter part 1.[31] In fluid-bed systems, transport lines for solids, etc. heavy erosion may occur. This type of attack has been shown to comprise two types of wear, one caused by repeated deformation during collisions, eventually resulting in breaking loose of a piece of material, the other caused by the cutting action of the free-moving particles. In practice these two types of wear occur simultaneously. Formulae could be derived expressing erosion as a function of mass and velocity of the impinging particles, impingement angle and mechanical and physical properties both of erosive particles and eroded body.

$$\text{€=Wd }/1/2M(V\sin\theta\text{-k})^2 \qquad (1.11)$$

Where Wd is deformation wear at normal impact condition, 'M' is the total mass of impacting particles, 'V' is velocity of particle, θ is impact angle and k is the normal component of particle impact velocity needed to initiate the erosion which is generally neglected, considering very small compared to the impact velocity.

If a particle strikes a horizontal surface at an acute angle, the material is subjected to shear over an area equal to the vertical cross section of that part of the particle which has penetrated into the surface. If the shearing strength is exceeded, destruction occurs. This type of wear was called cutting wear. In actual practice where every possible impact angle may occur the two forms of wear generally occur simultaneously. In the case of hard and brittle materials cutting wear is negligibly small in relation to deformation wear, whereas for soft and ductile materials the reverse may be true.

J.G.A. Bitter part 2.[32] It was stated that in erosion two types of wear are wear due to repeated deformation (W_d) and cutting wear (W_C), For deformation wear the flow equation was found:

$$\text{Wd= € x } 1/2M(V\sin\theta\text{-k})^2 \qquad (1.12)$$
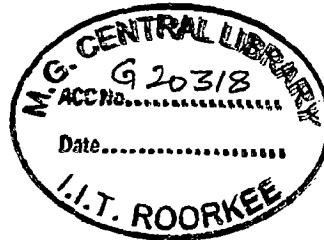
In which Wd = units volume loss, M= total mass of impinging particles, V = practical velocity, α = impact angle, K = maximum particle velocity at which the collision still is purely elastic and €= the energy needed to remove a unit volume of material from the body by deformation wear (deformation wear factor)

$$\text{W}_C\text{=m(V}^2\text{-v}^2)/2£ \qquad (1.13)$$

In which m = mass of the particle, (v) =the particle still has a horizontal velocity component when it leaves the body surface, £= the cutting wear factor.

20

1.7 OBJECTIVES OF THE PRESENT STUDY

The problem of erosion due to silt in Indian hydro power station is found to be quite serious, especially in those located in the Himalayan region. Erosion is a function of different parameters such as silt size, hardness, concentration, quantity, shape, velocity and the base material property. In most of the cases, this can be minimised by controlling the above mentioned parameters. During monsoon season it becomes impossible to control these parameters which cause erosion. Experimental and analytical lot of studies has been carried out to discuss the silt erosion in hydro turbine. It is very difficult to study all these parameters simultaneously by practical approach and that is time consuming also. So Finite Element Method (FEM) approach has been considered under the present study. FEM approach is less time consuming and provides more relevant information about erosion.

The present study having the following objective

   a) To study the erosion process.

   b) To find out erosion rate with varying velocity rate.

   c) To find out erosion rate with varying angle of impact.

CHAPTER -2

SILT EROSION IN HYDRO TURBINES

2.1 GENERAL

Erosive wear of hydro turbine runners is a complex phenomenon, which depends upon different parameters such as silt size, hardness and concentration, velocity of water and base material properties The efficiency of the turbine decreases with the increase in the erosive wear and final breakdown of hydro turbines Erosion due to impact of hard and abrasive particles is common phenomenon in hydro turbine under water parts and many other industrial situations. Extensive investigations have been carried out in the past to identify the factors responsible for severe erosive damages in hydro turbine underwater parts due to attack from silt laden water. A number of operating variables such as the impact angle and impact velocity affect the erosion process The rate of erosion is influenced by the relative hardness of the target material and the particles impacting on the surface .Ductile materials during erosion are considered to loose material through a cutting and ploughing mechanism at a low impact angle ,On the other hand, erosion damage of brittle materials is based on cracking, fragmentation and removal of flakes The erosion mechanism in terms of mechanical properties was presented by Bitter , He described that during impact, when the yield strength of the materials is locally exceeded, plastic deformation takes place in the vicinity of the impact. After multiple impacts, a plastically deformed surface layer may form near the eroded surface and, therefore, the yield strength of the material increases due to work hardening. Sundararajan and Shewmon suggested that during erosion material loss from a metal surface occurs when a critical fracture strain is achieved at the surface.

It was found that erosion rate depends mainly on the velocity of erodent particles and on the angle between the target surface and particle trajectory (impact angle). Further, it was revealed how other parameters (i.e., particle size and shape, their concentration, abrasive to target hardness ratio and the effect of liquid and solid additives) can change the nature and result of the process of erosion.

a) mium can lead to fracture problems that nullify the benefits of the hard surface.

2.2 PROBLEM OF EROSION IN HYDRO TURBINE

In India, 80% of available Hydro resources are from Himalayan region. Silt erosion of Hydro turbines is a widely acknowledged problem. Problem is severe in the Himalayan region because the mountains are young and relatively fragile. Silt and damage depend on nature of silt, quartz rich with quartz content generally 65%-95%, PPM content high: 5000 to 20000 in monsoon, Freshly broken fine conical particles. Due to silt damaged areas guide vane and Cheek plate, runner inlet at blade skirt and crown, runner outlet on pressure side, pelton nozzle & Spear, pelto runner bucket. Fig. 2.1 sowing the damaged caused due to silt in runner, guide vane and other part of hydro turbine

(i) Damaged runner   (ii) Close up of damaged runner blade

(iii) Damaged guide vane   (iv) Damaged seal drum

(v) Damaged top cover   (vi) Damaged lower ring
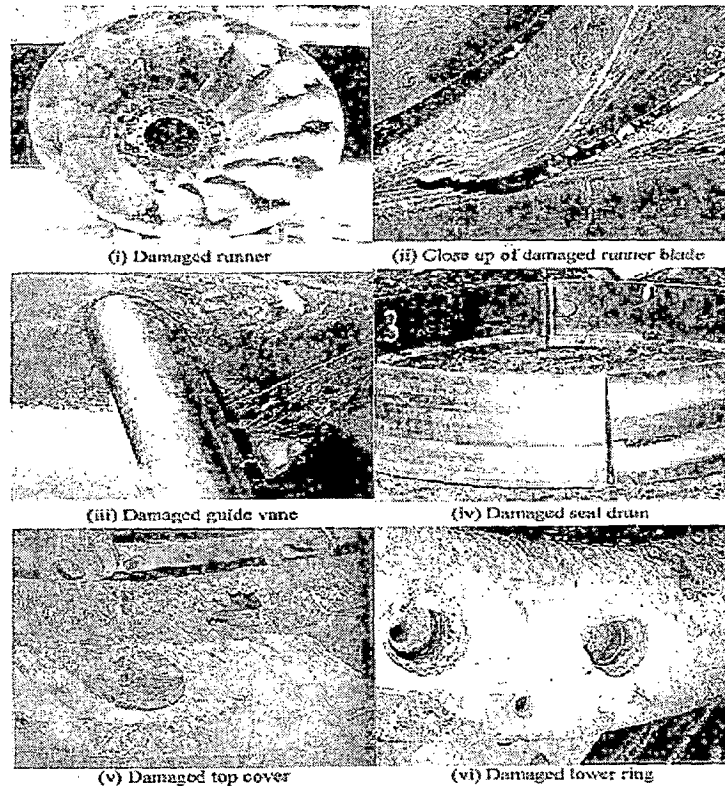
Fig. 2.1 Damage of turbine component due silt at site[8]

The reduction of the erosion is linked to the reduction of the velocity and therefore the size of

the turbine increases. This result in a higher price of the turbine, but it will reduce the maintenance costs during its lifetime. It has been shown from the above calculation that the design of the runner can decrease the sand erosion. If a Francis turbine designer combines the hydraulic design and coating of the critical parts, a significant reduction of erosion fig.2.2 and fig.2.3 sowing the damage in Kaplan runner and the guide vane.

Fig. 2.2 Severely damaged Kaplan runner by the impact of silt [6]
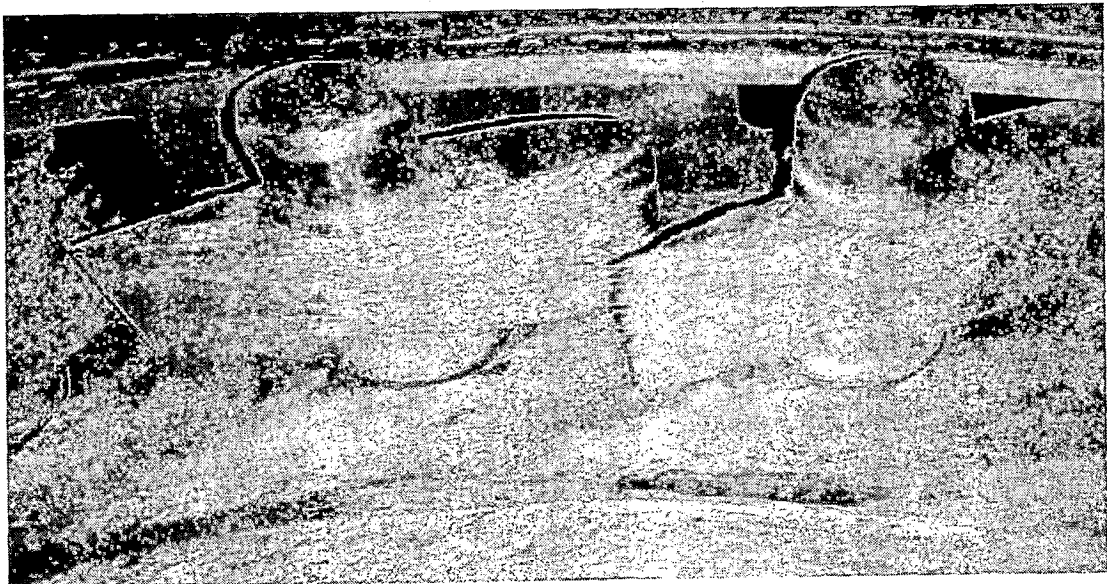
Fig .2.3 Silt erosion damage on the guide vanes [6]

Fig. 2.4 showing the variation in turbine efficiency with respect to varying load at different amount of silt content as silt content is low efficiency is high for the same load in jhimruk project
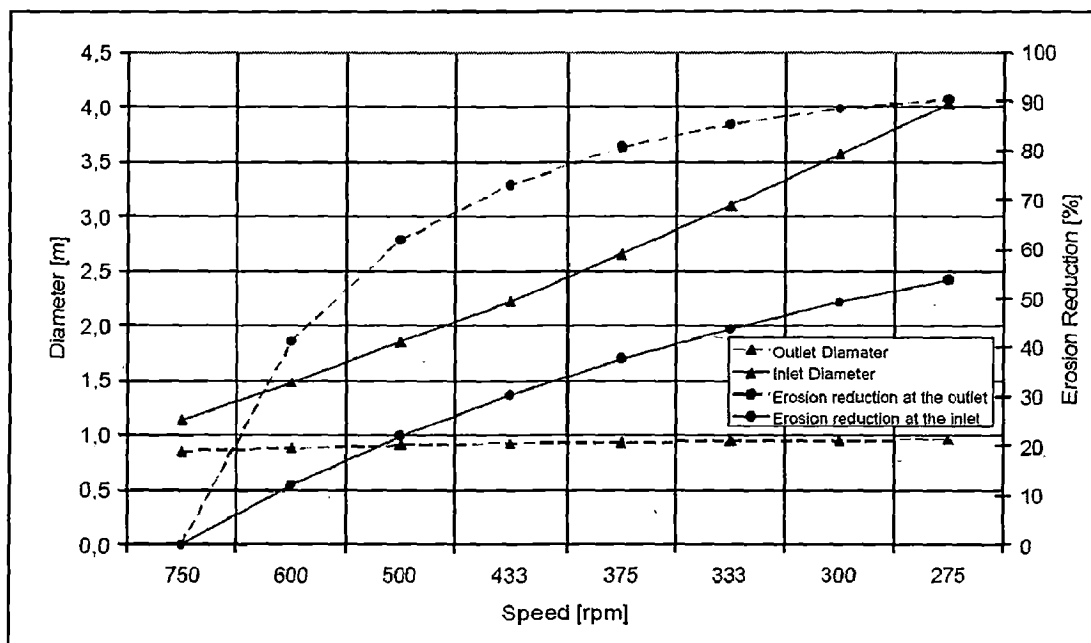
Fig.2.4 Results from the new design of the Francis runner

2.3 METHODS TO CONTROL WEAR

Wear can be prevented or minimized by reducing the intensity of wear through design, using wear-resistant material coating by thermal spraying, for example, nickel & iron based alloy. Nickel-based alloys are being widely used because they display good resistance to wear, oxidation and high temperature corrosion, as well as being low cost.

Erosive wear control steps.

a) Make the wearing surface hard through the use of hardfacing, vapor deposition techniques or high-energy processes (e.g., ion implantation).

b) Make the wearing surface resistant to fracture. Many wear processes involve fracture of material from a surface; thus toughness and fracture resistance play a significant

role in wear-resistant surfaces. The use of very hard materials such as ceramics, cemented carbides.

c) Make the eroding surface resistant to corrosion. Examples include the use of cobalt-base hardfacing alloys to resist liquid erosion, cavitation, and slurry erosion; nickel-base hardfacing alloys to resist chemical attack; and epoxy-filled rebuilding cements used to resist slurry erosion in turbines.

Silt erosion is a result of mechanical wear of components on account of dynamic action of silt flowing in the water coming in contact with the wearing surface. However The mechanism of erosion is complex due to interaction of several factors like sediment particles size, shape, hardness, velocity, impingement angle, concentration, properties of material and so on. The silt laden water passing through the turbine is the root cause of silt erosion of turbine components which consequently leads to a loss in efficiency thereby output, abetting of cavitation , pressure pulsations , vibrations , mechanical failures and frequent shut downs Since silt erosion damage is on account of dynamic action of silt with the component, properties of silt, mechanical properties of the component in contact with the flow and conditions of flow are therefore jointly responsible for the intensity and quantum of silt erosion. Therefore silt characteristic, velocity of silt laden water are the important factors to understand erosion intensity or extent of damage on hydro turbines.

2.4 SILT PARTICLE EROSION MECHANISM

Broadly there are two abrasive erosion mechanisms according to which a silt particle can attack the target or hydro turbine

    a) Gouging

    b) Hammering

Gouging is a tangential attack by the eroding body. Its action is equivalent to the action of a tool. To resist this, the material should be as hard as possible and not allow a crack to spread. Hammering is a normal attack by the eroding body. Its action is equivalent to a series of hammer blows. To resist this type of action, the material again has to be as hard as possible, and has to prevent the spreading of cracks. Thus abrasive erosion can be considered

as a combination of the two phenomena described above, with the eroding particle moving at considerable speed.

Material removal by Erosion may consist of any of the three mechanisms

a) Abrasion

b) Hammering

c) Impinging.

Metal removal by erosion/abrasion of various components is either by shearing-off of the metal by hard & sharp silt particles or by cracking and breaking of parent metal due to impact of the silt particles. Of the two, removal of metal by shearing-off is the major cause of erosion. . The shearing of metal can be reduced to a large extent if the particles do not hit the components at a high velocity and large angle of attack.

As it is known that silt particles attacks on the surface of the hydro turbine as a stream of solid particles so erosion of a surface by a stream of silt particles can be examined by considering the arrival times of the particles on the surface. For this treatment first a concept, an 'impact zone' is proposed, and then considers the arrival of the particles on one zone as a queuing process. The rate of erosion of ductile metals can then be predicted using simple arguments from probability theory.

2.5 FACTORS RESPONSIBLE FOR EFFECTING INTENSITY OR SIIT EROSION RATE

2.5.1 SILT CHARACTERSTICS

The physical properties of sand particles may be defined in many ways, such as grain size (equivalent diameter), shape (round or sharp edges), geological structure mainly hardness) and grading (distribution of varying sizes) and concentration. The intensity of erosion is directly proportional to the size of the particles. Particle sizes above 0.25mm are extremely harmful. It has been found that particles larger expressed in parts per million (ppm). Its cut-off values for damage to be significant are: 200 ppm for low and medium head machines (up to 150 m) and 150 ppm for high head machines than 0.25 mm, even with a hardness of less than 5 on Moh's scale, cause wear. Similarly fine silt (less than 0.1 mm) containing quartz can erode under water components. Fine silt is especially dangerous if the

27

turbine is operating under a high head. Sharp and angular particles causes more erosion compared with rounded ones the intensity of erosion is also directly proportional to the hardness of the particles (irrespective of their size). Particles with Moh's hardness of more than 5 are harmful. Himalayan silt is 90 per cent (7 on Moh's scale compared with 10 for diamonds). The silt concentration is the most dominating factor influencing erosion intensity linearly. It is generally expressed in parts per million (ppm). Its cut off values for damage are: 200 for low and medium head turbine (upto 150m), and 150 ppm for high head machines.

2.5.2 Velocity of silt-laden water

The intensity of erosion is usually proportional to the cube of the velocity V of the water carrying silt particles in suspension. This is particularly true for Francis runners. Any decrease in velocity, therefore would substantially reduce erosion damage. For instance, a 10 per cent decrease in water velocity could reduce erosion by 27 per cent.

2.5.3 Machine flow pattern

Intensity of silt abrasion is closely related to the local flow pattern in a machine i.e. same specimen materials can suffer different degrees of damage when placed in different locations with different types of flow. On the other hand, same type of abrasion can occur for each kind of material when placed at different locations, but with the same type of flow pattern.

2.5.4 Power Plant design criteria

Intensity damage due to silt at different power stations may vary even where silt conditions are identical which clearly indicates that equipment design has a significant role to play in influencing the intensity of erosion . Power plant design necessarily includes water passage, rotation speed and number of runner blades etc .

When a turbine is designed to handle high concentrations of silt, selection of a conservative specific speed is advisable. The adverse effect of silt is reduced in oversized machines. The rotation speed should be lower than the synchronous speed selected for a machine to be used in clean water. Experience also shows that design optimization is possible to mitigate silt erosion of critical zones. From the basic principles of hydrodynamics, the

energy transfer by hydrofoils results from their angle of incidence, curvature and shape. These parameters create differential velocities over the blade surface, and the rate of change of velocity depends on the curvature and length of the blade. It has been found that the peak velocity can be moderated by increasing the blade length, and the wearing life can be increased by increasing the thickness of the blades, especially towards the tip section. The turbine runner needs to be designed taking account of the following boundary conditions:

i. minimum curvature of the blade profiles towards the tip in the case of Kaplan units, and towards the outlet edge nearer the skirt in the case of Francis machines;

ii. point of maximum curvature as near as possible to the inlet edge in the case of Francis units and near to the hub in the case of Kaplan units, as well as reduction of curvature towards the outlet edge in both cases;

iii. minimum angle of incidence;

iv. long blade profiles and a flat rear section;

v. minimum number of blades; and,

vi. blade profiles to be as thick as possible with appropriate thickness distribution.

2.6   SILT EROSION RATE

By combining the above factors Silt erosion rate (W) can be expressed mathematically as

$$W \propto C_1 C_2 C_3 C_4 M_r V^x \qquad (2.1)$$

C_1 = Coefficient of silt concentration;

C_2 = Coefficient silt hardness;

C_3 = Coefficient of silt particle;

C_4 = Coefficient of silt particle shape;

M_r = coefficient of wear resistance of base material; and

V = velocity of water.

The following values of the exponent x are suggested:

3 for Francis runners; 2.5 for vanes and pivot ring liners; 2.5 for Pelton nozzles and 1.5 for Pelton runner buckets

2.7 ABRASION CRITERION FOR HYDRAULIC TURBINES

The product of operating head H and content of harmful sediments S_d (d>0.05mm) that essentially represents the energy content of the particles is selected as a measure of abrasion intensity. $HS_d = 7$ is roughly the dividing line between moderate damage and serious damage.

2.8 TURBINE EFFICIENCY IN SILTY WATER

It is important for new machine designs to undergo appropriate model testing with silty water to determine efficiency. The turbine efficiency is extremely sensitive to increased clearances between the guide vanes and their holding rings, besides runner labyrinth clearances. Even before any wear has taken place, the overall efficiency in silty water is reduced in proportion to the solids content. Hydraulic performance tests on a Francis turbine model with sediment- laden flow, conducted in Japan, showed that the turbine's best efficiency decreased almost in direct proportion to the increase in solids concentration or the specific gravity. The reduction in peak efficiency (η) is expressed as:

$$\eta_m = (1 - 0.085\ C_w)\ \eta_w \tag{2.2}$$

η_m= turbine peak η with sediment laden flow (mixture);

η_w = turbine peak η with clean water; and,

C_w = fraction of solids by weight.

The critical cavitation coefficient was also found to be influenced by the presence of silt in the flow; it increases in direct proportion to the mixture concentration at each unit speed

2.9 THEORIES FOR EROSION MECHANISM

To understand the mechanism of erosion on hydro turbines by silt particles we can take help of the various mechanistic theories developed for the material removal when a ductile metal target is eroded by solid particles (usually harder than the target) which are described as follows.

(i) Erosion by cutting: Finnie , Hutchings , Hutchings *et al* ,

(ii) Erosion by deformation wear: Bitter (a, b).

(iii) Erosion by target melting: Neilson and Gilchrist , Smeltzer *et al*,

(iv) Erosion by delamination wear: Suh , Jahanmir .

a) Erosion by cutting has been observed using high-speed photography by Hutchings ; it is the result of a sharp cornered projectile machining a chip of material from the target surface. Each impact leading to the removal of a chip is considered to be independent and the total amount of erosion is the sum of the contributions from each micromachining impact. This theory, which evolved from the study of the machining process on lathes, is both quantitatively and qualitatively successful. However, not all eroding particles are angular and not all impacts give rise to detached chips of material and therefore this theory appears to be unable to deal with these exceptions.

b) When a projectile impinges upon the surface of a ductile target it loses some kinetic energy. Most of this lost energy is transformed into plastic deformation and then into heat within the target. If this heat is generated sufficiently quickly and within a small enough volume of the target then the temperature there can reach the melting point. Target material can then be removed more easily due to its much reduced cohesive strength.

c) Suh's theory of abrasion by delamination wear has been extended by Jahanmir to include erosion. The target is considered to be composed of a matrix containing harder inclusions. The projectile interacts with the surface by sliding across it but not directly removing material. Delamination can only occur when subsurface cracks start to extend parallel to the target surface. These cracks are nucleated by voids which can form at the interface between the matrix and the inclusions. In order to nucleate a void, there must be present around an inclusion both a large shear stress and a large hydrostatic stress. This latter stress is not present initially. However, repeated sliding across the same portion of the target surface apparently

31

gives rise to large residual stresses and these are considered to be the source of the hydrostatic stresses. Clearly, the mechanism of delamination is a cooperative effect.

d) Bitter (a, b) assumed that the removal of material from the surface of a target occurs by the joint action of two mechanisms: cutting, which only occurs when the projectile strikes the target at grazing incidence; and deformation wear, which predominates at normal impingement. Unfortunately he did not explain clearly how material was removed by deformation wear. It may be that it is low-cycle fatigue (Hutchings) or, indeed, delamination wears. However, Jahanmir discusses delamination in terms of a projectile sliding across a surface and sliding is impossible at normal impingement.

Bitter (a, b) was careful to point out that deformation wear is characterized by repeated bombardment, by which he implies that it is a cooperative mechanism.

2.10 ANALYSIS OF SILT PARTICLE MECHANISM

F is the erosive flux; it is the silt mass rate crossing unit area of orifice. Throughout this work it will be assumed that F is constant. Clearly, $G \propto Ft$ and $W \propto M/t$. The erosion rate is not by definition equal to the time derivative of the mass loss (dM/dt) but if the loss of mass was to increase linearly from $t = O$ then $dM/dt = M/t$ and the erosion rate graph would become a straight line parallel to the time axis. Fig. 2.5 indicates that this behavior is obtained but only after the incubation period has passed,

Unfortunately, Uuemois and Kleis do not indicate what form Fig. 2.5(b) takes at short times. Experimental errors are relatively large at short times when the mass losses are smallest and it is common to see this portion of the curve omitted. The curves in figures 2.5(a) and (b) were both obtained from experiments performed at constant flux, In the discussion that follows models are presented which generate mass loss curves. The complementary erosion rate is as calculated and both curves are plotted which will give the shape of the curve as shown in graph. Examining theoretically the influence of time and flux on the loss of mass from a target with to the primary mechanisms. The concept of 'impact zone' associated with the impact of a single projectile is used and following this, there is a discussion of the queuing theory for the arrival of projectiles on one impact zone.

32
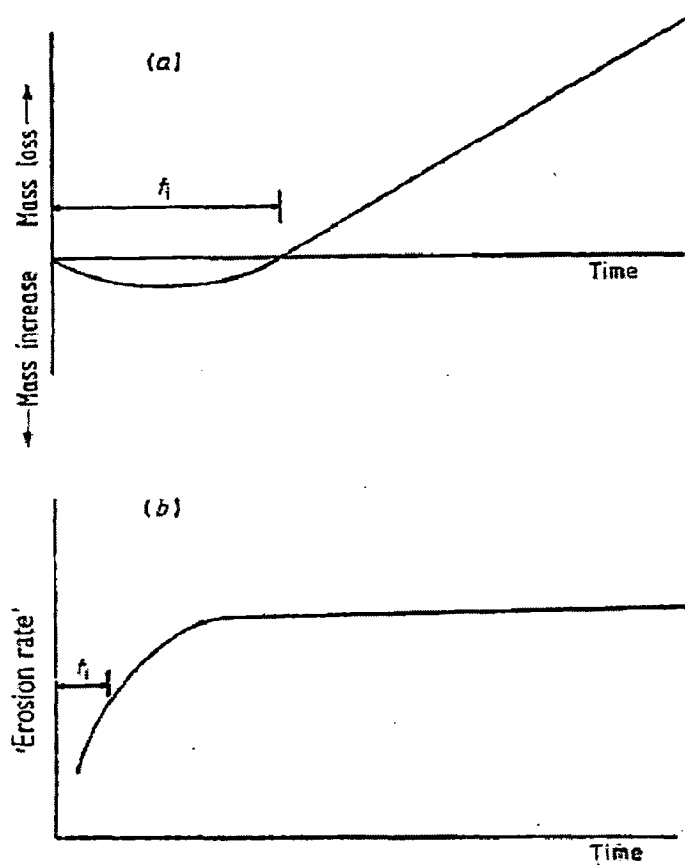
Fig, 2.5. *(a)* Change of mass of an eroded target with the duration of the test (typical behavior). After an initial period of incubation *ti* a linearly increasing mass loss is established (after Tilly). *(b)* Variation of 'erosion rate' (relative erosion) with time of test for a metal target (typical behavior). The plateau region is an indication that a constant rate of erosion has been established. (After Uuemois and Kleis .)

2.10.1 Concept of impact zone

The impact zone is the zone of plastic deformation around an impact site. If a precise measure of the zone size is required, it is best measured rather than estimated. This can be done by firing only a few particles at a virgin target surface so that there is little chance of

zones overlapping. The procedure which follows averages over many zones so that the error resulting from variation of the size of the impact zones becomes unimportant.

The impact zones are also considered to be non-interacting; erosion occurring on one zone does not influence the rate at which material is removed from adjacent zones. All zones are considered to be identical and edge effects are neglected. The datum point for time is taken as the commencement of the erosion test. The average number of particles per second striking one zone, Ω, (the zone impact frequency) equals Fσ/m. However, if the arrival of particles is random then the probability of an impact occurring inside some small time interval (t_1, $t_1+\delta t$) is simply $\Omega\delta t$. This probability is unaffected by the pattern of events before time t_1. If δt is chosen to be small (i.e. $\delta t<1/\Omega$) then the probability that two or more impacts will occur within (t_1, $t_1+\delta t$) is negligible. As these are the conditions of a Poisson process, it follows that the arrival of projectiles on to an impact zone is described by the Poisson distribution,

$$P(r) = \left[(\Omega t)^r / r!\right]\exp(-\Omega t)$$ (2.3)

r = number of impacts in (0,t).

The mean μ of the Poisson distribution is a standard result:

$$\mu = \Omega t$$

To calculate the loss of mass from one impact zone in the time interval (0, t) it is necessary to equate the loss of mass to the number of particles striking one zone during that interval. It is at this point that any cooperative effect of the impacts of projectiles becomes important. Using the above equation it is straightforward to calculate the expected mass loss from one zone (and hence from the whole target) using one linking mass loss equation.

2.10.2 Mass loss equations

Each impact is treated as an independent event and it is assumed that every impact removes the same (average) mass, m_c, of material from a zone. Expected mass loss, M_z from one zone in (0, t)

$$M_z = m_c \sum_{r=0}^{\infty} r[(\Omega t)^r / r!] \exp(-\Omega t) \qquad (2.4)$$

The equation can be simplified to give

$$M_z = m_c \Omega t \qquad (2.5)$$

Multiplying by the number of impact zones on the target, the expected mass loss, M, from the whole target in time (0, t) becomes

$$M = (A/\sigma) \, m_c \Omega t \qquad (2.6)$$

Or in terms of the total flux F

$$M = FA(m_c/m) \, t \qquad (2.7)$$

The erosion rate W associated with the mass loss can be found by dividing by the total mass of particles striking the target in time t (i.e. *FAt*).

$$W = M/Fat = m_c/m = \text{constt} \qquad (2.8)$$

This model describes the erosion characteristic of a process involving only independent impacts. Into this category fall the cutting mechanism and the independent melting mechanism of erosion. To improve this further the impacts are considered not be independent and it is assumed that the loss of mass from a zone cannot commence until the number of impacts exceeds a value which depends on time.

Now the expected mass loss from the target

$$M = \frac{A}{\sigma} m_m \sum_{r=r'}^{\infty} (r - r')[(\Omega t)^r / r!] \exp(-\Omega t) \qquad (2.9)$$

And the rate of erosion can be given by

$$W = \frac{m_m}{Fat} \sum_{r=r'}^{\infty} (r - r')[(\Omega t)^r / r!] \exp(-\Omega t) \qquad (2.10)$$

35

Cooperative melting requires that heat is generated in the surface of the target at a sufficient rate to raise the target temperature to the melting point and to maintain it at this level.

Thus by using the idea of an impact zone it is possible to treat statistically the arrival of particles on the surface of the target. It is not only easier to visualize erosion on one impact zone it is also straightforward to determine the loss of mass from that zone using simple probability theory.

2.11 SILT EROSION

As mentioned earlier, the extent of material removal depends on the velocity and force with which the particles act over the surface if blade curvature is relatively high, the resulting higher centrifugal force on the particles increases the intensity of erosion. Over a period of operation in silty water the surface becomes irregular, which, in turn induces local cavitation. Subsequently the destruction is faster as a result of the combined effects a turbine component completely free from cavitation when operating in clean water is affected by cavitation in silty water. Furthermore, a component already eroded by silt erosion is much more prone to cavitation pitting. The combined effect can be very severe and can be understood as follows With the hydraulic design parameters adopted these days (high specific speed), cavitation is considered to be largely responsible for the initiation of damage. Generally, removal of metal from a runner (excluding other underwater parts), is limited to 0.1 D^2 kg per 1000 h of operation, where D is the throat diameter of the runner in meters. For the sake of economy in manufacturing costs of turbines and generators, manufacturers do permit limited cavitation to take place. Turbine settings are thus fixed by the manufacturers, so that cavitation remains within the guaranteed limits. Some restrictions on operating conditions are also imposed. The above is generally based on the assumption that turbines will be operated in fairly clear water and thus no major damage is expected.

When cavitation does take place, the affected area develops pumiceous and honeycomb like pits, and the metal is weakened. Because of this, the water flow is locally disturbed. If the water is clean, there is generally no serious problem as a result of this limited cavitation. However, when silt-laden water passes over this, the spongy area is rapidly removed as a

result of sliding abrasion. The fresh runner area develops a similar pumiceous spongy surface (from cavitation) and is again removed by the grinding action of the sand, which is present in the water. The rate of removal depends on the size, hardness, roughness, silt concentration and velocity of the water. Thus, the outlet edges of the turbine blades, where velocities are higher, become thinner. Vibration takes place and, as a result of fatigue, cracks develop and ultimately, pieces of the runner wash out. The lost pieces of the runner blade greatly disturb the flow condition, and severe damage occurs.

If the turbines operate in clear water, it takes a much longer time for the water to remove the cavitation-affected spongy areas. The presence of silt accelerates the damage. The damage caused by a combination of cavitation and abrasion is therefore much more rapid and severe compared with damage caused by either of them separately. Some well-known facts about cavitation erosion and sand abrasion are:

· The viscosity of particle-laden flow is higher than clear water, especially when the water contains very fine grains such as ash and clay. As the critical vaporizing pressure is raised, the inception of cavitation is delayed.

The intensity of cavitation erosion is related to the velocity of the flow in the sixth power or higher.

The intensity of sand erosion is roughly proportional to the third power of flow velocity.

There is an evident incubation period with cavitation erosion. The rate of damage may be identified with stages of incubation, acceleration, deceleration and equilibrium. Sand erosion has no incubation period damage is simply proportional to time.

Damage to metal surfaces where there is interaction between cavitation and erosion is much more serious than each attack alone.

COMPUTATIONAL ANALYSIS OF SILT EROSION IN HYDRO TURBINE MATERIALS

3.1 GENERAL

Problem of erosion due to silt in a number of Indian hydro power stations is found to be quite serious, especially in those located in the Himalayan region. Erosion is a function of different parameters such as silt size, hardness, concentration, quantity, shape, velocity and base material properties. In most cases, this can be minimized by controlling the above-mentioned parameters. During monsoon season, it becomes impossible to control these parameters which cause erosion. So, it is essential to know their effects. Wear, which occurs due to low and high-energy particle impact, can be controlled by velocity or by controlling silt size, shape and concentration. The low energy impact wear can also be controlled by providing suitable hard coatings. However, this becomes critical for high particle impact wear. An experimental study was undertaken for understanding its nature. In this study, hard coatings such as hard chrome plating, plasma nitriding, D-gun spraying and boronising were studied for high-energy impact wear resistance. Boronising appears to be excellent for this, followed by D gun sprayed WCq12Co coating. Based on this experimental study, boronising is being field-tried on a component which is prone to erosion due to high-energy particle impacts. Under identical test conditions at high particle impact energy, the borided T410 steel performed much better than D-gun sprayed tungsten carbide as well chromium carbide, hard chrome, plasma nitriding and boronised 13Cr–4Ni steel. The borided T410 steel is free from cracks and voids. The microstructures of D-gun sprayed tungsten carbide and chromium carbide show a few voids and oxides as defects. At high particle impact energy, thes defects could cause deterioration of the coating. The microstructure of borided 13Cr–4Ni steel also has defects such as cracks and these extend deep inside the coating up to the base and are responsible for unsatisfactory performance. The microstructures of hard chrome and plasma nitrided samples are free from all these defects. However, they lack the resistance to abrasive wear as their microhardness values are below the threshold values of the microhardness values of the erodent 1100 Borided T410 steel appears to be an excellent

erosion resistance shield to combat highenergy particle impact wear. It can provide an appropriate solution to the hydropower stations severely affected due to silt and coming under categories A and B. Other coatings such as D-gun based, hard chrome and plasma nitriding may not provide an appropriate solution. This is because of their unsatisfactory performance in the laboratory.

3.1.1 ANALYSIS INVESTIGATION IN PAST

Experimentally, one may measure volume loss or weight loss of a material and investigate the erosion mechanism by analyzing the worn surface and the erosion conditions. A lot of researches about the erosive wear have been done by Finnie, Bitter, Hutchings, Barkoula and Karger-Kocsis . Meng has provided information about 28 erosive wear models and prediction equations in his doctoral dissertation. And from the 1990s, the computational methods were used in characterizing the erosive wear. Adler established the two-dimensional (2D) water drop impact model with DYNA3D code in 1995. The calculation did not involve any solid erodent. Shimizu simulated the 2D solid particle erosion (SPE) based on the plane strain assumptions. Chen and Li utilized a 2D micro-scale dynamic model (MSDM) investigated the effect of particle shape on erosive wear. Li examined the deformation behavior of Al particles impacting on Al substrate using the arbitrary Lagrangian-Eulerian (ALE) method in 2D. The 2D simulation has advantages of fine meshes and less computation time

Bitter defined erosion as "Material damage caused by the attack of particles entrained in a fluid system impacting the surface at high speed" while Hutchings wrote "Erosion is an abrasive wear process in which the repeated impact of small particles entrained in a moving fluid against a surface results in the removal of material from that surface. Removal of material occurs through the processes of micro-plastic deformation and/or brittle fracture. For ductile materials such as pure metals and alloys, the impact of the hard particles causes severe, localized plastic strain at the impact site on the surface. Material is removed when the strain exceeds the material's strain-to-failure. For brittle materials, such as ceramic and intermetallic compounds, the force of the impacting particle causes localized cracking at the surface. With subsequent impact events, these cracks propagate and eventually link together, and as a result, material becomes detached from the surface. As a consequence, the particle

impingement angle on the surface affects each material in a different manner. Ductile materials exhibit maximum erosion rates at attack angles of about 20–40° while brittle materials exhibit a maximum erosion rate at an angle of 90°. No external forces act on the impacting particle other than the contact forces exerted by the work piece material surface. The contact forces are responsible for the deceleration of the impacting particle.

3.2 EROSION PROBLEM AND PRESENT STUDY

Erosion caused by slurry is a serious problem in hydro turbine. The rate of erosion are depends on

3.2.1 Impingement variables describing the particle flow:

    a) Particle velocity

    b) Angle of impact

    c) Particle concentration

3.2.2 Particle variables:

    a) Particle shape

    b) Particle density

    c) Particle size

3.2.3 Material variables (workpiece and particles):

    a) Young's modulus

    b) Poisson's ratio

    c) Plastic behavior

    d) Failure behavior

It is very difficult to study all these parameter in laboratory and also time consuming so taking this is in view here we are considering the FEM(Finite Element Method) approach to solve the erosion problem in hydro turbine materials. We use Johnson–Cook constitutive equation failure model for have been introduced in more details. The 2D Rigid Particle, axis-symmetric impact models with the failure element removal are employed in order to get computational efficiency and sufficient failure elements in characterizing the wear resistant materials and high speed erosion process. The effect of the impact angle, impact velocity on

the wear performance of 13cr-4Ni are discussed. The advantage of this method is that it includes element failure and element removal allowing the simulation of actual material loss. In this work element failure/removal method is used to model the erosion behavior of 13cr-4Ni

3.3 COMPUTIONAL ANALYSIS

To study the erosion problem in hydro turbine materials. The Johnson Cook material model was employed to model the flow stress behavior of the target workpiece material. In the Johnson-Cook model, as detailed in Eq. (3.1), the flow stress is expressed as a function of the strain ε, strain hardening index n, strain rate $\dot{\varepsilon}$, reference strain rate $\dot{\varepsilon}_0 = 1.0$ m/s., work piece temperature T, room temperature T_r, melting temperature T_m and strain-rate sensitivity index m.

$$\sigma_f = (A + B\varepsilon^n)\left(1 + C \ln\left(\frac{\dot{\varepsilon}}{\varepsilon_0}\right)\right)\left(1 - \left(\frac{T - T_r}{T_m - T_r}\right)\right) \tag{3.1}$$

A, B, and C are constants acquired experimentally by Leseur from compressive split Hopkinson bar tests in punching shear configuration on13cr-4Ni. The Johnson-Cook materials constants for 13cr-4Ni are detailed in Table3. 1.

3.3.1 FAILURE CRITERIA FOR HYDRO TURBINE MATERIAL

A shear failure criterion was incorporated in the material model to simulate material removal during the erosion process. The material failure strain ε_f is detailed in Eq.(3.2), as a function of non-dimensional plastic strain $\dot{\varepsilon}^p/\dot{\varepsilon}_0$, a dimensionless deviatoric-pressure stress ratio σ_p/σ_e (where σ_p is the pressure stress and σ_e is the Von-Mises stress), computed or modelled work piece temperature T, room temperature T_r, and melting temperature T_m.

$$\varepsilon_f = (d_1 + d_2\, e^{d_3(\sigma_p/\sigma_e)})\left(1 + d_4 \ln\left(\frac{\dot{\varepsilon}^p}{\varepsilon_0}\right)\right) \times \left(1 + d_5\left(\frac{T - T_r}{T_m - T_r}\right)\right) \tag{3.2}$$

The damage occurs when the damage parameter $D = \sum \varepsilon/\varepsilon_f$ reaches the value of 1. For the explicit dynamic finite element method, the target material has been dispersed many small finite elements, and through the dynamic calculation, the$(\sum \Delta\varepsilon)i$ of every element is

calculated. For arbitrary element i during each time step, when its damage parameter $D_i = 1$, the element i was marked failure and removed from the model immediately.

Table.3. 1 J-C Material constants of ductile materials[6]

Materials properties	Symbol	13cr-4Ni
Shear modulus	G (GPa)	41.9
Young's modulus	E(GPa)	110
Poisson's ratio	N	0.31
J–C yield strength	A (MPa)	1098
J–C hardening coefficient	B (MPa)	1092
J–C strain hardening exponent	N	0.93
J–C strain rate constant	C	0.014
J–C softening exponent	M	1.1
Melting temperature	Tm (K)	1878
Specific heat	Cp (J/(kg K))	580
J–C damage constant	d1	−0.09
J–C damage constant	d2	0.27
J–C damage constant	d3	0.48
J–C damage constant	d4	0.014
J–C damage constant	d5	3.87

Generally, the erosion rate (mg/g) was used to characterize the erosion performance of the target materials. It is defined as .

$$\text{Erosion rate} = \frac{\text{Cumulative mass loss of target materials(mg)}}{\text{Impact particles weight(mg)}}$$

3.3.2 IMPACTING PARTICLE MATERIAL

The impacting-particle material simulated as spherical abrasive particles with a density of 3900 kg/m^3 with a size of 120μm and total mass of 3.52E-9 kg. The dimensions of axisymmetric substrate is 1mm x 0.5mm. In the finite element model, the impacting-particle material is modeled as a rigid body (stresses and strains are assumed to be zero in the impacting particle material.)

3.4 METHODOLOGY TO SOLVE THE EROSION PROBLEM

Modeling of the erosion process was performed using a general purpose, commercially available, Finite Element Solver; ABAQUS/EXPLICIT (version 6.8). The analysis employed a Lagrangian formulation. details the momentum equation[3.3].

$$MU' = F^{ext} - F^{int} \qquad (3.3)$$

Where M is the lumped mass matrix, U' is the nodal acceleration at each time step, F^{ext} is the externally applied load for each node and F^{int} is the internal force. This set of equations is solved using explicit time integration with the central difference method employing a lumped mass matrix, which improves the computational efficiency considerably. A modified central difference with velocity and acceleration computed at half time step is used, as detailed in Eq. (3.4)

$$U^{(i+(1/2))} = U^{(i-(1/2))} + \frac{\Delta t^{(i+1)} + \Delta t^{(i)}}{2} U^{(i+(1/2))} \qquad (3.4)$$

The explicit procedure require a time increment less than the critical time increment Δt_{cr} (otherwise the solution becomes numerically unstable). Δt_{cr} can be computed using Eq. (3.5),

$$\Delta t_{cr} = \frac{L_e}{\sqrt{\frac{E}{\rho(1+\nu)}}} \qquad (3.5)$$

where Le is the length of the element, E is the young modulus of elasticity, ρ is the material density and v is the Poisson's ratio.

3.4.1 CONTACT ALGORITHM

Contact is defined between the impacting-particle and the target workpiece. In ABAQUS /EXPLICIT, a contact surface pair consists of two surfaces that are expected to come into contact during the response solution. The two contact surfaces are designated the master and slave surfaces. The outer surface of the impacting-particle is set as the master

43

surface, while the workpiece volume in the vicinity of impact is considered as the slave surface (region). The Coulomb friction relationship as detailed in Eq.(3.6) was used in the contact model[6][8]:

$$F_{f} = \mu F_{n} \tag{3.6}$$

where Ff the friction force, Fn is the normal force and m is the friction coefficient. Meo and Vignevic investigated the effect of friction coefficient magnitude and frictionless impact on residual stress field during shot peening process where the shots are made of hard steel while the work-piece is made of 13cr-4ni. From their analysis, it was concluded that significant differences were found on the residual stress profile between frictionless impact and an impact with 0.1 friction coefficient. However, the variation of the residual stresses and plastic strains is negligible for $0.1 < \mu < 0.5$. Therefore in this work, the Coulomb friction coefficient between indentor and workpiece material is assumed to be 0.4.

3.4.2 MESHING ELEMENTS

In order to achieve good results without extensive computations the workpiece is partitioned with finer structured mesh in the vicinity of the impact point and rest of the model is meshed coarsely. Explicit-Axisymmetric Stress, Linear Quad elements were used to mesh the target, while no meshing is done for the impacting particle due to rigid properties. Fig.3.1 and fig. 3.2 shows both meshing used in substrate and coating.
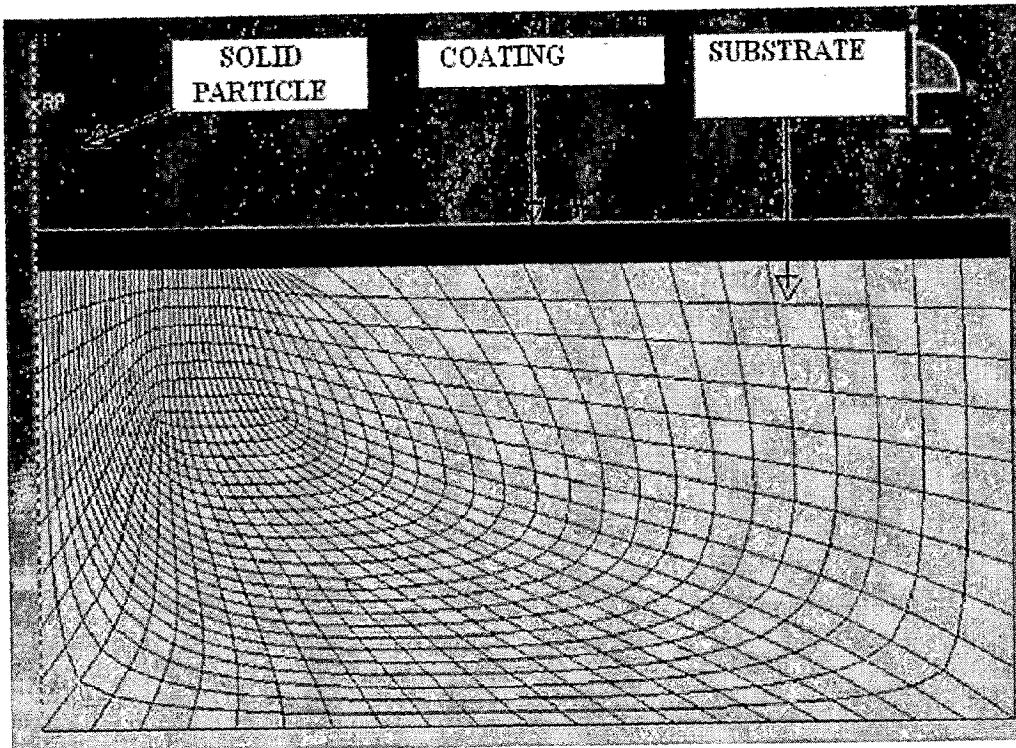
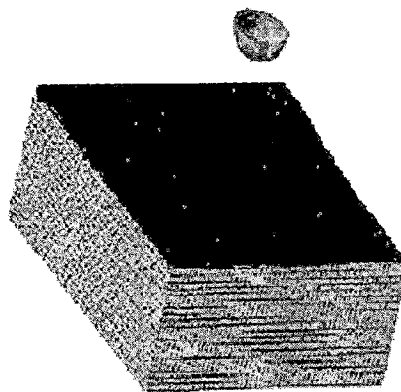Fig.3.1 Meshing for the finite element model.

Fig3.2Representation of FEM model in 3D.

3.5 TEST CONDITIONS

Table 3.2 gives an overview for two different cases studied in this work. The first case studies the effect of particle velocity on the erosion rate for five different velocities selected

45

in the range of 20–80 m/s which. The second case is a study on the effect of impact angle on the erosion rate; five models are used with impact angles, ranging from 30 to 90°.

Particle Velocity At Impact(m/s)	20		40		60		80
Impact angle $(\theta°)$	30	45	60		75		90

Table 3.2 Test parameter

Only a quater-model is evaluated and constrains are set at the boundaries to achieve the symmetry conditions. The bottom line is fixed and the particle are constrained from rotation around the X (1) and Y (2) axis as shown in fig.3.3 and fig3.4.
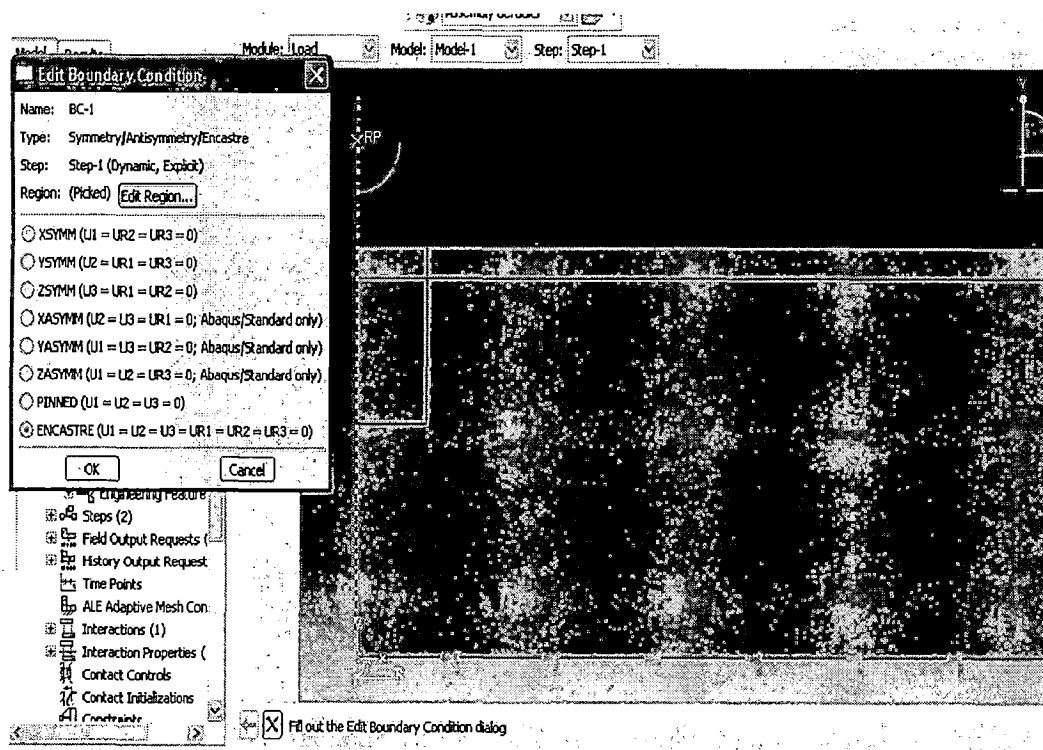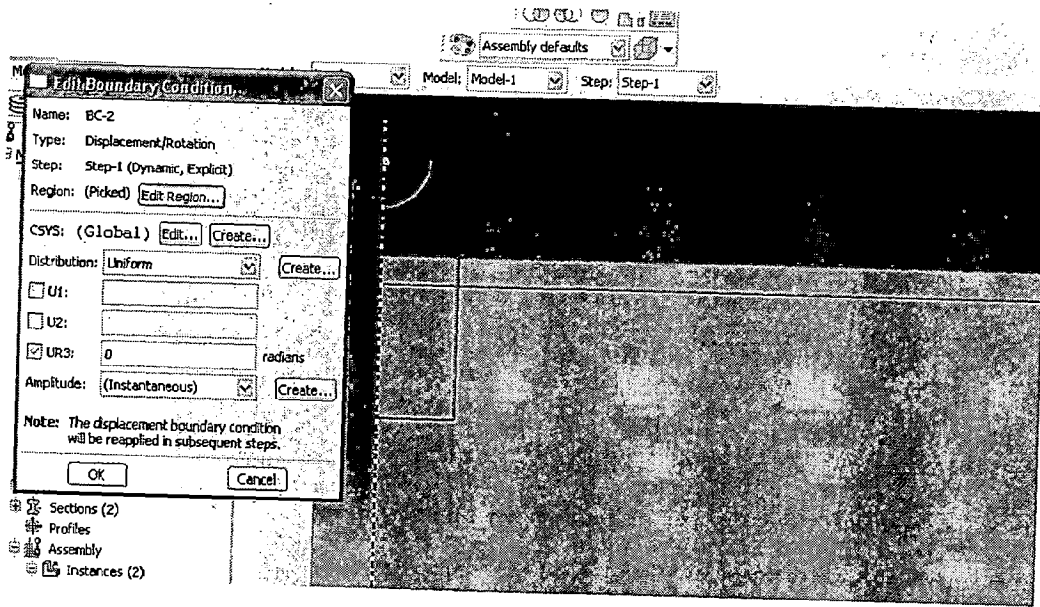
Fig.3.3 Fixing the Base Of Substrate.

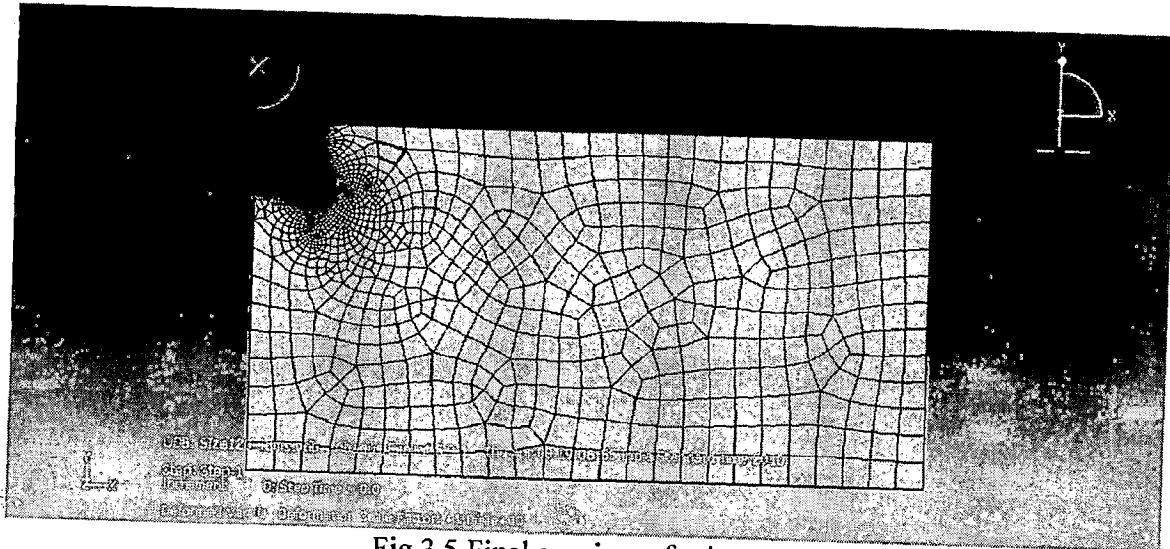Fig.3.4 Rotational D.O.F Of Particle is Set to Zero.

Fig.3.5 Final specimen for impact

3.6 RESULTS

3.6.1 Erosion Rate V/S Particle Impact Velocity

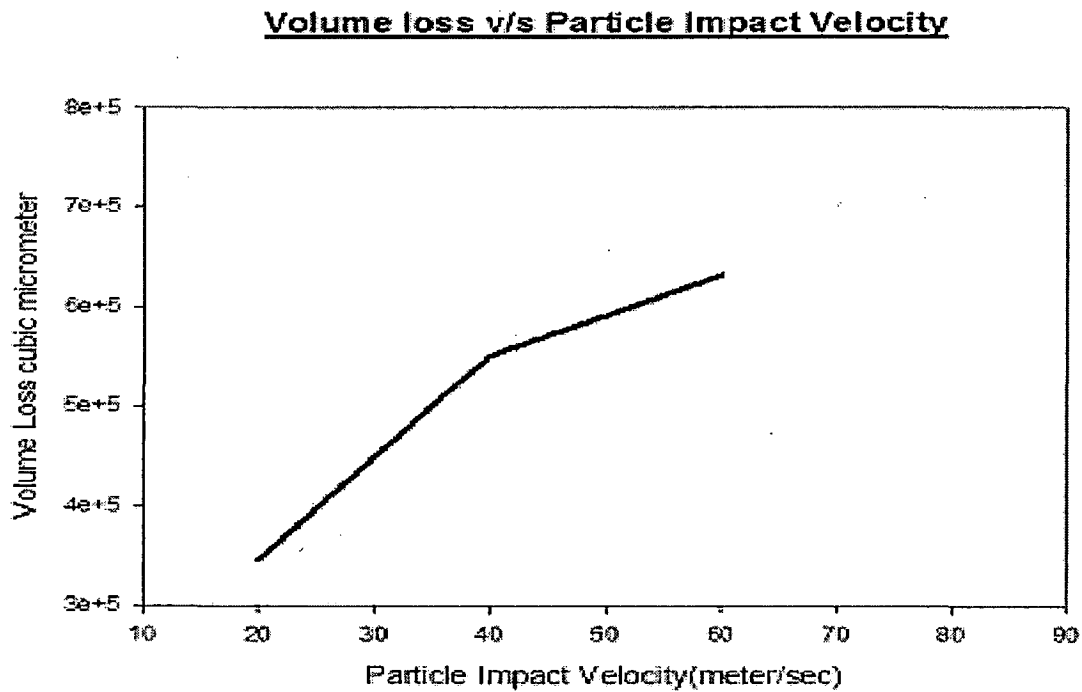**Volume loss v/s Particle Impact Velocity**

Fig 3.6 volume loss due to erosion v/s particle impact velocity

In the present study velocity considered is from 20-80 m/s, which is applicable for pelton turbine. The volume change rises linearly with an increased slope till 20-40m/s velocity, then the graph rises with comparatively lesser slope .This profile of graph is same as published in different studies of erosion.

3.6.2 Erosion Rate V/S Particle Impact Angle.

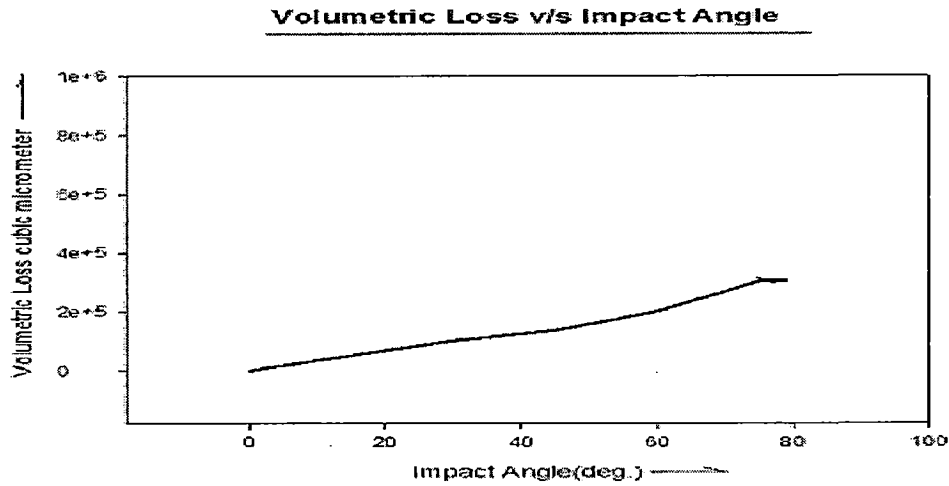**Volumetric Loss v/s Impact Angle**

Fig3.7 volume loss due to erosion v/s impact angle

From the graph we can conclude that as angle increases from 0-30° volume loses linearly. Then it increases exponentially in the range of 30-75°, afterward it increases linearly with sudden rise from 75-90°. We can conclude that maximum erosion takes place at 90°.Which verifies our results with others study

3.6.3 CHANGE IN ENERGY WITH RESPECT TO TIME

Fig.3.8 shows that kinetic energy decrease suddenly approximately 95% directly with the impact and the remaning will deacceleret with taking few sec.
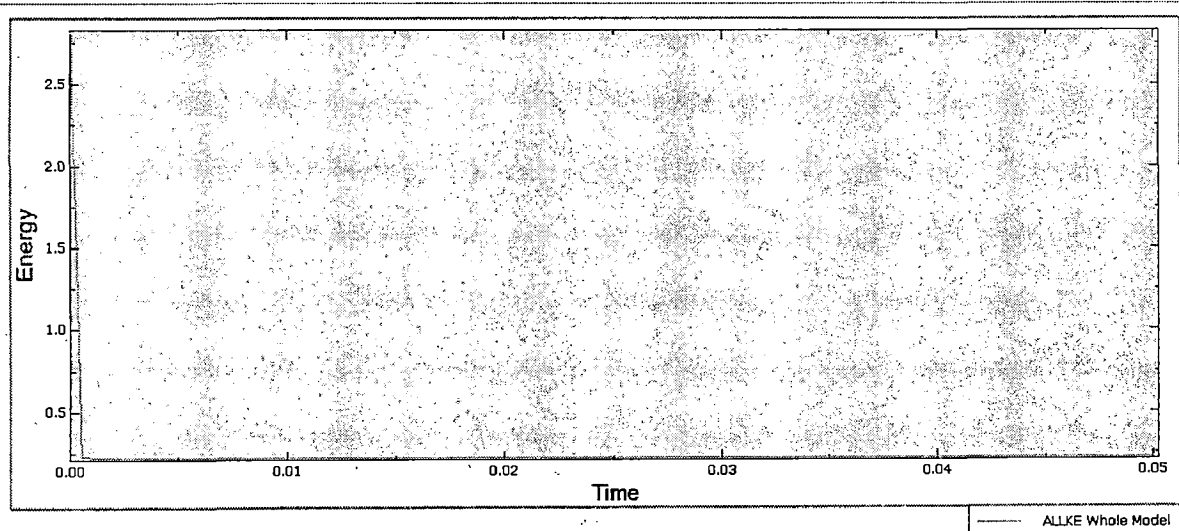

Fig3.8 change in kinetic energy with time during impact

The value of strain energy as shown in figure 3.9 increase linearly first then with a steep slope then it increase with lesser slope and at the point of failure it increase almost perpendicular to time
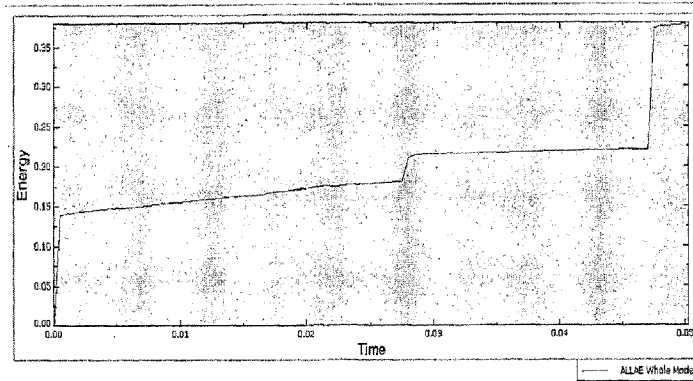

Fig3.9 variation of strain energy with respect to time

3.6.4 DISTRIBUTION OF STRESS IN PARENT MATEAL

Fig. 3.10 showing the distribution of stress in parental matel after the impact the different colour showing the intensity of stress at different point in material
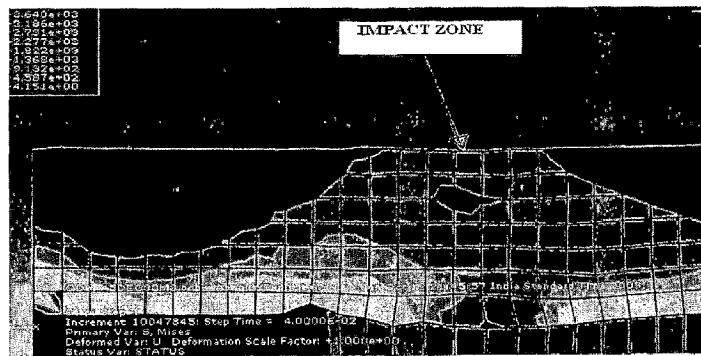

Fig.3.10 Distribution of the failure stress inside the parental material after impact

CHAPTER-4

EXPERIMENTAL PROCEDURE AND TECHNIQUES

4.1 GENERAL

The problem of erosion due to silt in a number of Indian hydro power stations is found to be quite serious, especially in those located in the Himalayan region. Martensitic stainless steels (alloy containing normally twelve percent chromium) have been in use for many years with principal applications in corrosive and elevated temperature environments.

The beneficial aspect of chromium in promoting the acid and oxidation resistance of irons and steels has been known for over a century. This knowledge was eventually transferred to the advancing technology of "stainless" steels in the early 1900's. With the invention of the thermit process for producing low-carbon ferrochromium early in the twentieth century, modest addition developments produced the first martensitic and ferritic stainless steels (eleven percent Cr or more), which were closely followed by the austenitic varieties .

Many developments have occurred in martensitic alloys. From their early inception, these alloys had a wide variety of applications. The effects of alloying elements and processing could now be traced to the essential source of the properties developed; the microstructure of the material. Switzerland was apparently the first place where a low-carbon thirteen percent Cr steel bearing approximately four percent Ni and normally one-half percent Mo emerged . Shortly thereafter, AB Bofor's in Sweden developed a very similar grade, 2RM2, containing 13Cr6Ni . Several variations on these basic systems exist and commercial alloys of this type are available in many countries. Within the United States both cast and wrought product forms of the 13Cr-4Ni material are available as ASTM A296-79/A487 Grade CA6NM and ASTM A182-78 Grade F6NM respectively.

4.2 MATERIAL USED

The material used in this investigation is 13-4 martensitic stainless steel conforming to the specification ASTM A743 CA-6NM. The chemical composition of the martensitic stainless steel in weight % is as follows:

Composition percent max.								
C	Mn	Si	Cr	Ni	P	S	Mo	Fe
0.06	1.00	1.00	11.5-14.0	3.5-4.5	0.04	0.04	0.4-1.0	Balance

4.3 EROSION TEST

There are different methods which are used for erosion measurement in the academic or research centres around the world. These different methods are due to the different operating conditions.

In the most generalised way, three typical types erosion testing rigs can be considered on the basis of motion between mixture and specimen. They are: (i) jet/nozzle type (ii) rotating disc/arm type, and (iii) centrifugal accelerator type.

4.3.1 DESCRIPTION OF EROSION TESTING MACHINE

Erosion testing machine as shown in the fig. 4.1 also called as Slurry pot erosion tester. This machine consists of a container in which slurry was poured.

Fig 4.1 Schematic of slurry pot erosion tester.

52

The container was filled with slurry of concentration of 10 wt%. The slurry container contains four vertical baffle plates from inside to minimize rotational flow of the slurry bath. The spindle was driven by the electric motor (1440 rpm) with the help of V-belt giving an instantaneous cylindrical velocity of 3.18 m/s. The spindle contains central shaft which was attached to the sample holder. The central shaft can be adjustable at any vertical position through gear lever mechanism.

The sample holder contain two disc plates which were put close together by four bolt and nut arrangement, which help us to clamp the samples. To hold the samples at particular angles i.e. 30°, 60°, and 90° slots were cut at that particular angle (tangent with respect to the slurry) on both bottom and top of disc plates from inside as shown in fig to accommodate the samples.

4.4 TESTING METHOD

Most of the actives in the slurry erosion test are manual. All observations of the experiments were recorded manually. Briefly, the sequence of the test procedure is as follows:

    i. The specimen was prepared for the erosion test with the help of the belt grinder and polished on the emery papers 1/0, 2/0, and 3/0.

    ii. Cleaning the specimen with acetone.

    iii. Drying the specimen.

    iv. Note down the original length, breadth and weight of the specimen.

    v. Prepare the slurry in the container by adding 9 parts of the water and 1 part of the sieved sand.

    vi. Clamp the specimen in the sample holder at different impingement angles.

    vii. Attach the sample holder to the spindle, immerse it in the slurry and lock the spindle.

    viii. Start the machine and note down the time for operation.

    ix. Remove the specimen from the spindle and sample holder after stipulated time.

    x. Cleaning and drying the specimen.

    xi. Weighing the specimen after erosion.

Sand particles were sieved on Tyler testing sieves in a Ro-tap machine to obtain the size ranges of interest in the experiment. A sieved sand sample was used to prepare the slurry mixture for the experimental run.

To know the particle size distribution the sieve analysis was carried out. In the sieve analysis 500 gm. of sand was taken. The sieves were arranged as a column one over other. The coarsest meshing at the top and the finest at the bottom with gradually decreasing size of meshing. Sand was kept in the first sieve which had the coarsest meshing. It was made to shake all the sieves so that the sand settles down in the sieves of different meshing. The retained sand in each sieve was weighed and the particle size of the sand was calculated.

4.5 TEST VARIABLES

The range of parameters for the present investigation is given in table 1. For this purpose, mean particle size of 500μm was selected to conduct experiments at 3.18 m/s velocity and 10 wt % concentration.

Table 4. 1 Experimental parameters

Variables	Operating Conditions
Erodent material (1100 HVN)	Quartz
Mean particle size (μm)	500 (594-420)
Solid concentration (wt %)	10
Temperature	Room temperature

4.6 TEST RESULTS

The test results from the erosion experiment were presented in this chapter. The test was carried out for 14 hrs. Weight loss was measured after different stipulated time for each of the specimens. Cumulative weight loss was also calculated. The surface area of the specimen was calculated and was divided to the weight loss so as to calculate the weight loss in terms of the gm/mm^2, this would provide an easy way to compare and analyze the data. The erosion loss is now independent from the size of the specimen. Erosion rates are presented either as a ratio of weight loss of material to exposure time (hrs) or volume loss of specimen to exposure time (hrs). Normally erosion rate of coatings are presented in terms of ratio of volume loss to

weight of particles. The erosion behaviour of as received specimens has been studied. The initial dimensions and weight of various specimens are reported in table 4.2. The experimental result pertaining to the weight loss and cumulative weight loss in slurry erosion tester at different angles are reported in table4. 3. The cumulative weight loss was calculated in terms of weight loss per unit surface area and is presented in table 4.4.

Table 4.2 Initial Data of Erosion Test Samples of 13-4 martensitic stainless steel

Specimen specification	Length 'l' (mm)	Breadth 'b' (mm)	Thickness 't' (mm)	Weight (gm)	Surface area (mm²) = 2[(l*b)+(l*t)]
30°	19.98	10.75	5.44	8.7921	646.95
60°	20.00	10.73	3.57	5.7234	572.00
90°	19.98	10.81	5.45	9.0101	649.75

Table 4. 3 Erosion Data of As Received 13-4 martensitic stainless steel in erosion test

Impingement angle	30°		60°	
Time (hr)	Wt. Loss (gm)	Cum. Loss (gm)	Wt. Loss (gm)	Cum. Loss (gm)
0	0	0	0	0
1	0.0081	0.0081	0.0471	0.0471
2	0.0043	0.0124	0.0023	0.0494
3	0.0032	0.0156	0.0008	0.0502
4	0.0011	0.0167	0.0008	0.0510
6	0.0012	0.0179	0.0007	0.0517
9	0.0022	0.0201	0.0003	0.0520

14	0.0015	0.0216	0.0005	0.0525
Total Wt. loss (gm)	0.0216		0.0525	

Table4. 4 Cumulative weight loss in terms of weight loss per unit surface area of 13-4 martensitic stainless steel

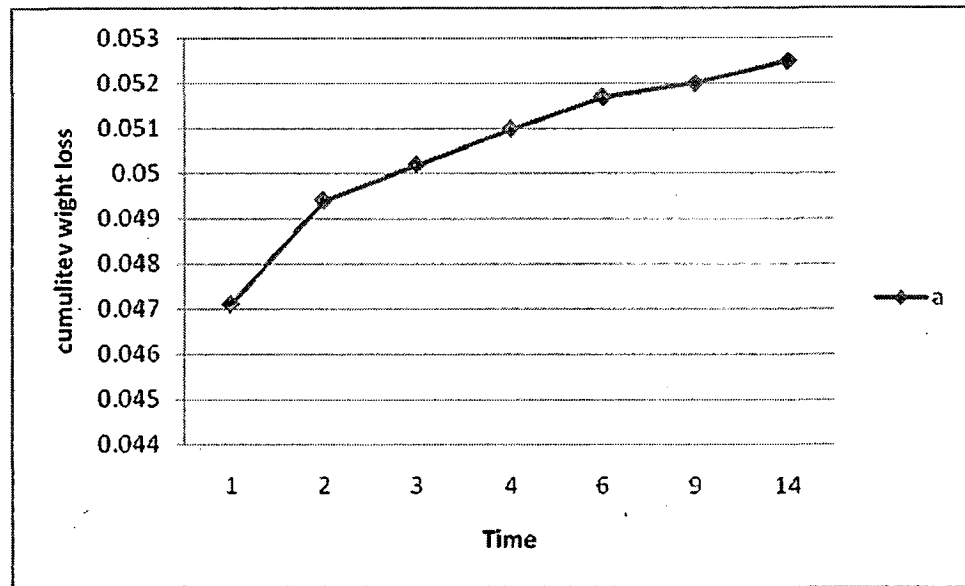| Specimen specification	Cumulative Weight Loss (10^{-5} gm/mm^2)							
	0 hr	1 hr	2 hr	3 hr	4 hr	6 hr	9 hr	14 hr
30°	0	1.25	1.92	2.41	2.58	2.77	3.11	3.34
60°	0	8.23	8.64	8.78	8.92	9.04	9.09	9.18

Fig.4. 2 Cumulative weight loss vs. erosion test duration for different impact angle
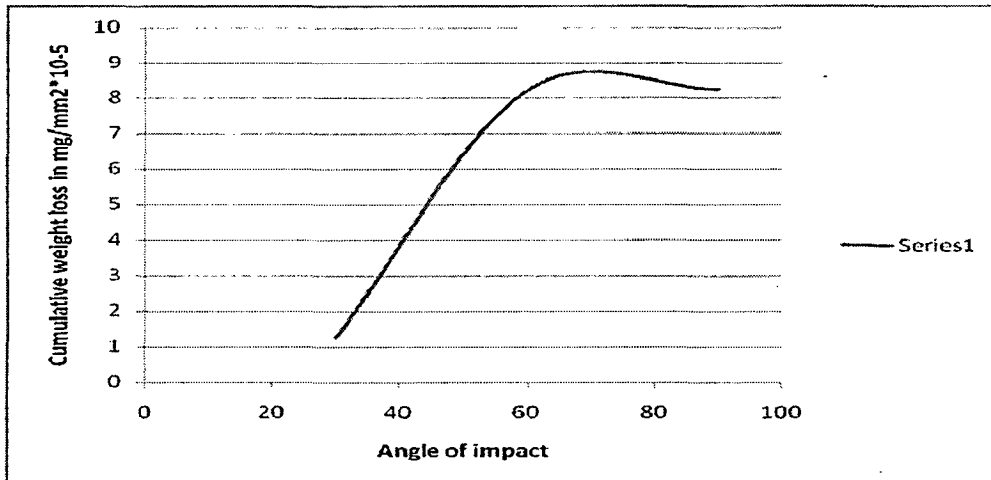
Fig 4.3 cumulative wt loss v/s angle of impact

Fig.4.3 having the same profile as our fig 3.7 in chapter 3 which shows that the simulated result are matching with practical work that sow the validation of this work with the practical work.

CONCLUSIONS AND RECOMMENDATIONS

5.1 CONCLUSIONS

The present study the erosion rate of the turbine material under different velocity of impact and impact angle has been investigated using Finite Element Method and also by experiment. In order to analysis the erosion rate of turbine material 13Cr-4Ni ABAQUAS/EXPLICT software has been used the parameters range impact velocity from 20 m/s to 80 m/s and the angle of impact range from 30 degree to 90 degree have been considered. From the study following conclusions are drawn.

i. It has been found that in the velocity range from 20-80 m/s, which is applicable for pelton turbine. The erosion (volume change) rises linearly with a higher rate up to 40m/s velocity, then this volume change occur at lower rate . It further concluded that as the impact angle increases from 0-30° volume loses linearly. Then it increases exponentially in the range of 30-75°.

ii. An experimental study has also been carried out for the validation of analyzed results for a specimen of 13Cr-4Ni on the slurry pot machine.

iii. Based on comparison of result it has been found that analysis result are comparable with experimental results.

5.2 RECOMMENDATIONS

Future study may be conducted with variations in size of slurry particles.

REFERENCES

[1] Asthana B.N., Seminar on 'Silting problems in hydro power stations'. WRDTC, Roorkee, India, Determination of optimal sediment size to be excluded for run-of-river project a case study (May 1997).

[2] Schneider. C and Kachele. T Conference proceedings silting problems in hydro power plants, New Delhi, India, on Recent research results on predicting and preventing silt erosion (1999).

[3] Mack R, Drtina P, Lang E. Numerical prediction of erosion on guide vanes and in labyrinth seals in hydraulic turbines. Wear 233(1999), pp68–91.

[4] Keck H., Dekumbis R. and Sick M. ,Sediment erosion in hydraulic turbine and experiences with advanced coating technologies, India Hydro 2005; International workshop and conference may (2005).

[5] Chattopadhyay. R, High silt wear of hydro turbine runners, Wear 162–164 (1993), pp. 1040–1044

[6] Chauhan Akhilesh , Goel .D .B and Satya Prakash, Erosion behaviour of hydro turbine steels, Bull. Mater. Sic., volume 31, april 2008,pp115-120

[7] Neopane Hari Prasad ,Ole Gunnar Dahlhaug and Thapa Bhola , Alternative Design of a Francis Turbine for Sand Laden Water. International Water Power Dam Construction April (1998), pp. 36–37

[8] Pande V. K, Hydro-abrasion of water turbines in Himalayas. In: Conference. of CBIP, Jun 1987

[9] Mann .B.S, Particle erosion a new concept of flow visualization and boundary layer investigations of rotating machines at high Reynolds numbers, Wear 237 (2000), pp. 140–146

[10] Padhy Mamata Kumari and Saini. RP. A review on silt erosion in hydro turbines, Renewable and Sustainable Energy Reviews 12 (2008), pp. 1974–1987

[11] http://www.tev.ntnu.no/vk/publikasjoner/pdf/ArneKjolle/chapter14.pdf .

[12] Neilson JH and Gilchrist A. Erosion by a stream of solid particles. Wear 1968:pp 111-121.

[13] Bain AG and Bonnington ST. The hydraulic transport of solids by pipeline. at Oxford: Pergamon Press 1970, pp 131–6.

[14] Krause M and Grein H. Abrasion research and prevention. Journal Hydropower and Dam1996, pp.17–20.

[15] Naidu BSK. Addressing the problems of silt erosion at hydro plants. Hydropower and Dams 1997,pp72–76.

[16] Padhy Mamata Kumari and Saini. RP, Effect of size and concentration of silt particles on erosion of Pelton turbine buckets, Energy volume34, issue 10, October 2009,pp 1477-1483.

[17] Takgi T, Okamura T and Sato J. Hydraulic performance of Francis turbine for sediment-laden flow. Hitachi revie No-2, 1988.

[18] Sundararajan GA , comprehensive model for the solid particle erosion of ductile material. Wear 1991, pp.111–127.

[19] Roman JM, Xin LY, Hui WM, and Reginensi JP. Dealing with abrasive erosion in hydro turbine. Hydropower and Dams 1997, pp.67–71.

[20] Mann BS, Arya V. Abrasive and erosive wear characteristics of plasma nitriding and HVOF coatings: their application in hydro turbines. Wear 249(2001),pp.354–60.

[21] Engelhardt M, Oechsle D. Smooth operator. Water Power Dam Jun 2004.

[22] Thapa B and Brekke H. Effect of sand particle size and surface curvature on erosion of hydraulic turbine. In:22nd IAHR symposium on hydraulic machinery and systems November 2004,

[23] Ahluwalia MS and Gaur BK. Review of measures for minimising damages in hydro plants from excessive silt in river water. In: Workshop on: Silting problems in hydro electric power stations, CBIP, 1987.

[24] Singh SC. Operational problems and development of a new runner for silty water. Water Power Dam Constr1990,November,pp.29–37.

[25] Yan MZ. Protecting hydro turbines in silt-laden rivers. Hydropower and Dams 1996,pp.22–34.

[26] Kumar A and Tyagi SK. Problem of erosion of underwater parts due to heavy silt in Ganga Valley PowerStation. Selected papers: Silt damages to equipment in hydro power stations and remedial measures, CBIP,New Delhi, July 1996.

[27] Prasad G, Mathur GN and Agrawal AB. Silt erosion of generating equipment—case study of Salal and Baira Siul power station of NHPC. In: Seminar on: Silting Problems in Hydro Power stations. WRDTC, Roorkee, India, May 1997.

[28] Wood J. An answer to abrasion. International Water Power Dam Construction 1998;April, pp.36–47.

[29] Pradhan PMS, Improving sediment handling in the Himalayas. OSH research, Nepal, October 2004.

[30] Thapa B, Strestha R, Dhakal P and Thapa BS. Problems of Nepalese hydropower projects due to suspended sediments. Aquatic Ecosystem Health Manage 2005,pp.251–257.

[31] Bitter J.G.A., part 1, A study of erosion phenomena. part I and II, Wear 6 (1963) 5–21, 90–169.

[32] Bitter J.G.A., part 2, A study of erosion phenomena. part I and II, Wear 6 (1963) 5–21, 90–169.

[33] www.powermin.nic.in- Ministry of power, Govt. of India.

LIST OF PUBLICATIONS

1. Kuldeep Singh Shekhawat, Dr. R.P.Saini and Dr. Arun Kumar, "**Finite Element Method (FEM) Analysis of Silt Erosion in Small Hydro Turbine**" National Seminar on Advancement of Renewable Energy, presented at Arya College of Engineering, Jaipur,

2. Kuldeep Singh Shekhawat, Dr. R. P. Saini and Dr. Arun Kumar "**Advance FEM Analysis of Erosion**", abstract selected at Maulana Azad National Institute of Technology, Bhopal, for International Conference on Renewable Energy.